sustainable chemistry

MDPI

Article

Sustainable Grinding Performances of Nano-Sic Reinforced Al Matrix Composites under MQL: An Integrated Box–Behnken Design Coupled with Artificial Bee Colony (ABC) Algorithm

A. Nandakumar [1], T. Rajmohan [1], S. Vijayabhaskar [1] and D. Vijayan [2,*]

[1] Centre for Composite Science and Tribology, Kanchipuram 631561, India
[2] Department of Mechanical Engineering, Sri Chandrasekharendra Saraswathi Viswa Maha Vidyalaya, Enathur, Kanchipuram 631561, India
* Correspondence: vijayand@kanchiuniv.ac.in

Abstract: The presence of abrasive particles in ceramic reinforced composite materials makes the machining complicated by generating friction at elevated temperatures. Lubricants can be used to prohibit the hazard of higher temperatures. This research work is focused on examining the effects of lubricants on the grinding performances of Al matrix composites reinforced with nano-SiC particles under minimum quantity lubrication (MQL). A cylindrical grinding machine is used to perform the grinding experiments by employing a Box–Behnken design. Multiple performances, such as surface roughness, grinding forces and temperature, are optimized by considering the depth of cut, speed of the workpiece, wheel speed and wt % of nano-SiC using response surface methodology (RSM)-based artificial bee colony (ABC) algorithm. Atomic force microscope (AFM) and scanning electron microscopy (SEM) are used to observe the morphologies of the machined surfaces and the wheel.

Keywords: grinding; minimum quantity lubrication; Box–Behnken design; artificial bee colony (ABC) algorithm; atomic force microscope; scanning electron microscopy

check for updates

Citation: Nandakumar, A.; Rajmohan, T.; Vijayabhaskar, S.; Vijayan, D. Sustainable Grinding Performances of Nano-Sic Reinforced Al Matrix Composites under MQL: An Integrated Box–Behnken Design Coupled with Artificial Bee Colony (ABC) Algorithm. *Sustain. Chem.* **2022**, *3*, 482–510. https://doi.org/10.3390/suschem3040030

Academic Editor: Maria L. Auad

Received: 17 September 2022
Accepted: 9 November 2022
Published: 14 November 2022

Publisher's Note: MDPI stays neutral with regard to jurisdictional claims in published maps and institutional affiliations.

Copyright: © 2022 by the authors. Licensee MDPI, Basel, Switzerland. This article is an open access article distributed under the terms and conditions of the Creative Commons Attribution (CC BY) license (https://creativecommons.org/licenses/by/4.0/).

1. Introduction

At present, sustainable manufacturing has become an emerging environmental, economical, societal and technological challenge to the industry, academia and government entities [1]. Sustainable development is an important issue for many fields, including production, industry and manufacturing. However, in modern production, there has been increasing attention directed toward careful selection of proper cutting fluids from the viewpoint of cost, ecology and environmental issues [2].

The usage of metal matrix composites (MMCs) is increasing in both aeronautical and automotive industries [3]. The successful and cost-effective machining of MMCs is essential for the production of flawless items possessing improved surface finish and the required dimensions. The grinding process might play a significant part in hard machining and finishing operations, where a single grinding operation signifies a financial alternative, by eliminating the necessity for conventional machining processes, such as milling and turning [4].

Even though various ceramic reinforcements were found suitable for MMCs, Silicon carbide (SiC) has received increased attention owing to its dimensional stability, stiffness, high specific strength, wear resistance and high hardness [5]. The machining of SiC reinforced composites presents substantial difficulties for manufacturing because of the non-homogenous and anisotropic structure of the reinforcing particles along with their high abrasiveness. Early tool failure is proclaimed as a critical issue in the machining of MMCs [6]. The usage of traditional coolants to overcome these issues is an alternate option, even though unsuitability has been reported relative to traditional coolants in the machining

of composites [7]. While MMCs are preferred due to high capacity and machine-intensive mechanisms, it is crucial that the machinability of the materials is implicit. A feasibility study of grinding on nano-SiC reinforced Al matrix composites was performed under the influences of parameters including wheel speed, workpiece speed, depth of cut and wt % of nano-SiC [8].

In conventional machining processes, the technical efforts focused on the investigation of the grinding characteristics of metal matrix composites are inadequate [9–13]. In the grinding of SiCp/Al composites, a common problem is the formation of voids and delamination on the machined surface, which is due to reinforced particles being pulled out and aluminum matrix adhesion on the machined surface [14]. Optimizing the grinding process is a difficult task because the grinding wheel contains a large number of cutting edges, which are randomly spaced within the periphery of the wheel [15].

Surface finish and surface integrity are important for surface-sensitive parts subjected to fatigue or creep. Therefore, finishing processes, such as grinding, are utilized to marginally improve the surface integrity of machined MMNCs [16]. Dry cutting is preferred in the field of environmentally friendly manufacturing. However, these methods are less effective when higher machining efficiency, better surface finish and severe cutting conditions are required [17]. The minimum quantity of lubricant (MQL) concept in machining is an alternative to completely drying or flooding the lubricating system for reducing the amount of lubricant [18]. This calls for the applicability of MQL-based vegetable oil in the grinding of MMNCs.

Driven by the elevated cost of cutting tools, it is logical and attractive to optimize the cutting conditions, such as the effect of the cutting fluid. Currently, to reduce the adverse effects related to the usage of cutting fluids, researchers have established eco-friendly manufacturing, such as employing a cutting fluid based on vegetable oil with other cutting fluids in machining and minimum quantity lubrication (MQL) in machining [19].

The most important objective of the cutting fluid is to minimize the friction between abrasive work contacts by lubricating the whole machining zone [20]. The synthesized nano-fluids are effective in reducing the grinding forces and temperatures, especially in extreme machining conditions [21]. Nano-fluid-assisted MQL grinding obtained low grinding force ratios, specific grinding energies and surface roughness [22]. Optimal grinding results are obtained when the MQL nozzle is positioned at a 10–20° angle toward the wheel [23]. MQL can effectively reduce friction at the cutting interface, inhibit temperature rise, prevent adhesion, extend tool life and improve surface quality in machining processes, such as turning, milling, drilling and grinding [24].

Bin and Albert demonstrated that MQL grinding can achieve the same level of material removal rate without increasing the grinding forces compared to flood cooling [25]. Sethuramalingam et al. showed that the carbon nano-tube mixed with nano-fluid in the grinding process improved surface characteristics, such as surface roughness and micro-cracks [26]. The grinding forces are significantly reduced when a nano-cutting fluid is used, even at low concentrations of nano-particles, and surface finish was found to improve with higher concentrations of nano-particles [27]. MQL grinding reduces the grinding forces and specific grinding energy. As a result, the wheel wear is lowered with an increase in G-ratio. In addition, the surface generated by MQL grinding is smoother than fluid grinding and significantly better than dry grinding [28]. An improvement in tool life of almost 20–25% has been observed under minimum quantity lubrication (MQL) due to better cooling and lubricating effects. However, this effect is more prominent at a higher cutting speed of 150 m/min [29].

MQL grinding using vegetable oil achieved a lower friction coefficient, as well as specific grinding energy and grinding wheel wear compared to flood grinding [18]. MQL grinding in comparison to fluid cooling and dry grinding reduces the tangential forces considerably due to the presence of a lubricant around the grinding wheel, providing better slipping of the grain at the workpiece–tool interface [30]. Water-based Al_2O_3 nano-fluid MQL grinding can significantly reduce the grinding temperature, decrease the grinding

forces, improve the ground surface morphology and reduce the surface roughness in comparison to pure water MQL grinding [31]. Nano-fluid MQL grinding with higher concentration nano-particles has a lower grinding force, grinding temperature and surface roughness in comparison with lower concentration nano-particles [32]. Nano-fluid MQL is effective for reducing the grinding forces and enhancing surface quality. In addition, the size and volumetric concentration of nano-particles are critical parameters to influence the performances of the micro-grinding process [33]. The tangential cutting force is decreased with MQL, possibly due to the presence of a lubricant around the grinding wheel, providing better slipping of the grain at the workpiece–tool interface [34].

Sani et al. have studied the effectiveness of the modified neat Jatropha lubricant (MJO) while machining AISI 1045 steel orthogonally by using the MQL technique [35]. The experimental results revealed that MJO + AIL 10% and MJO + PIL 1% lubricant blends enhanced the machinability characteristics during the cutting process, thereby promoting a further sustainable and greener working environment. Krolczyk et al. have reviewed the hard-to-cut materials' machining ecological trends. They analyzed the ways of improving the machining processes through sustainable and cleaner production. The use of sustainability in machining resulted in an eco-friendly environment [9]. Li investigated the performance of graphene-based nano-fluids in the milling of TC_4 alloy applying MQL. The experimental results revealed that MQL machining improved the machinability characteristics of TC_4 alloy by employing enhanced cooling and lubrication [10]. Mia et al. have found that LN_2 dual jets improved the machinability characteristics of Ti-6Al-4V. It was observed that the optimized parameters mainly had a feed rate of 0.16 mm/rev and a cutting speed of 140 m/min during the cryogenic machining process [11]. Gajrani et al. have investigated the performance of a green cutting fluid based on vegetable oil in the turning of hardened AISI H-13 steel under MQL, flood and dry environments. The experimental results revealed that the machinability characteristics of the workpiece improved with the MQL technique in comparison with flood and dry machining [12]. Ni assessed the performance of water-based cutting fluids during the grinding disc cutting process (GDCP) of AISI 1045. The experimental results revealed that W-S-based cutting fluids can decrease the life span and cutting tilt by 34.5% and 14.8%, respectively, while enhancing the G-ratio by 77.6% when compared to cutting under dry conditions [36]. Stachurski et al. have studied the simultaneous introduction of a lubricant into the grinding zone by using MQL and compressed cooled air (CCA) during the grinding process of hob cutters' cutting blades. The experimental results revealed that the hybrid MQL–CCA method improves surface roughness by limiting the conventional coolant flow rate when compared with flood grinding [37].

Dogra et al. reviewed the eco-friendly techniques in grinding operations. They stated that MQL is a sustainable, cleaner production system during the grinding process, as it can enhance the heat transfer rate at the cost of a lower amount of coolants [38]. Zhang et al. have investigated the performance of a cryogenic air nano-fluid MQL (CNMQL) system during surface grinding of Ti-6Al-4V. It was revealed from the experiments that the CNMQL system obtained a minimum specific grinding energy of 51.96 J/mm^3 and a friction coefficient of 0.60 as compared to nano-fluid MQL and cryogenic air due to better grinding/lubricating mechanisms [39]. Rapeti et al. evaluated the influence of nano-fluids based on vegetable oil during the turning of AISI 1040 steel. Optimum results were obtained by employing gray relational analysis based on the Taguchi technique. The experimental results revealed that 0.5% nano molybdenum disulfide in coconut oil improved the turning performance at a feed rate of 0.14 mm/rev and a cutting speed of 40 m/min under MQL conditions [40]. Lee et al. have employed electrostatic lubrication assisted by the nano-fluid airflow (AF-ESL) technique during the micro-grinding operation in a titanium alloy. The experimental results revealed that nano-fluid AF-ESL can enhance the grinding characteristics of a workpiece at a nano-diamond particle size of 80 nm in the nano-fluids [41].

Pashmforoush and Bagherinia have studied the effect of copper nano-fluid based on water during Inconel 738 superalloy grinding. The performance measures of the

grinding process, such as surface roughness and wheel loading ratio, were evaluated by employing the image processing technique. The experimental results revealed that nano-fluids had improved the grinding performance significantly in comparison with conventional fluid grinding and dry grinding [42]. Mia et al. have investigated the effect of a solid lubricant, MQL and dry plain turning with compressed air-cooling techniques during the machining of hardened AISI 1060 steel. The experimental results revealed that the MQL technique improved the machinability characteristics of the workpiece, thereby providing environmental friendliness and cleaner production [43]. The outcome of the grinding process is influenced by many factors/parameters, and the design of experiments is used to identify the individual contributions of the parameters along with their intricate relationships [8]. Box–Behnken designs are response surface designs that have the prime benefit of addressing the problems involved in determining the experimental limits and specifically in preventing extreme treatment combinations [5].

The literature indicated that sustainable manufacturing appears to be a universal idea. Mitigating the vital elements in all areas, including machining processes and MQL-based nano-fluid lubrication, has demonstrated a significant decrease in the consumption of the cutting fluid as well as the cutting energy. A careful examination of the literature review revealed that only a minimal number of articles are available in the area of MQL-based grinding of MMCs. Therefore, this research focuses on examining the effect of lubricants on the grinding performance of nano-SiC reinforced Al matrix composites employing MQL. A cylindrical grinding machine is used to carry out the experiments applying a Box–Behnken design. Multiple performances, such as surface roughness, grinding forces and temperature, are optimized by considering the depth of cut, wheel speed, the speed of the workpiece and the wt % SiC nano-particles using an RSM-based artificial bee colony (ABC) algorithm. Atomic force microscope and scanning electron microscopy (SEM) are used to observe the morphologies of the machined surfaces and the wheel.

2. Materials and Methods

2.1. Material Used

Aluminum reinforced with SiC nano-particles is fabricated by a vacuum-based solidification process. The details of aluminum and nano-SiC used for the fabrication are given in Table 1. SEM with EDX and IR spectroscopy of nano-SiC reinforced aluminum matrix composites are shown in Figure 1. A uniform distribution of SiC nano-particles in the metal matrix nano-composites is observed. The micro-graphs predict that commercial nano-particles of silicon carbide will exhibit typical features that peak slightly below 800 cm^{-1}. This is a manifestation of the fundamental Si and C sublattice corresponding to the Reststrahlen band of the SiC single crystal observed in the range of 770 to 1000 cm^{-1} [44].

Vegetable oil based on cashew nut, SAE20W40 and Nano-TiO_2 bought from M/s Ganapathy traders, India, are used for this investigation. The ultrasonic processor is used to mix 500 mL of cashew nutshell oil and 10 g of Nano-TiO_2. Prior to the property measurements, the blended samples are maintained ideal for 24 h. The measured nano-fluid properties are presented in Table 2. The heat-carrying ability of the nano-fluid increases as the flash and fire points increase. The diameter of the wear scar and the image of the wear scar on the ball surface are measured using a TR-30L-IAS four-ball tribometer. The wear tests are carried out at a regular load of 148 N, speed of 1200 rpm and lubricant temperature of 75 °C [45]. Specific image capture software is used to measure the diameter of the wear scar and to obtain the wear scar image on the ball surface. The wear scar diameter is very low in cashew nutshell oil + TiO_2 compared to that of SAE20W40 and cashew nutshell oil. It is evident from Figure 2 that the wear scar image of cashew nutshell oil + TiO_2 is smoother, more precise and circular.

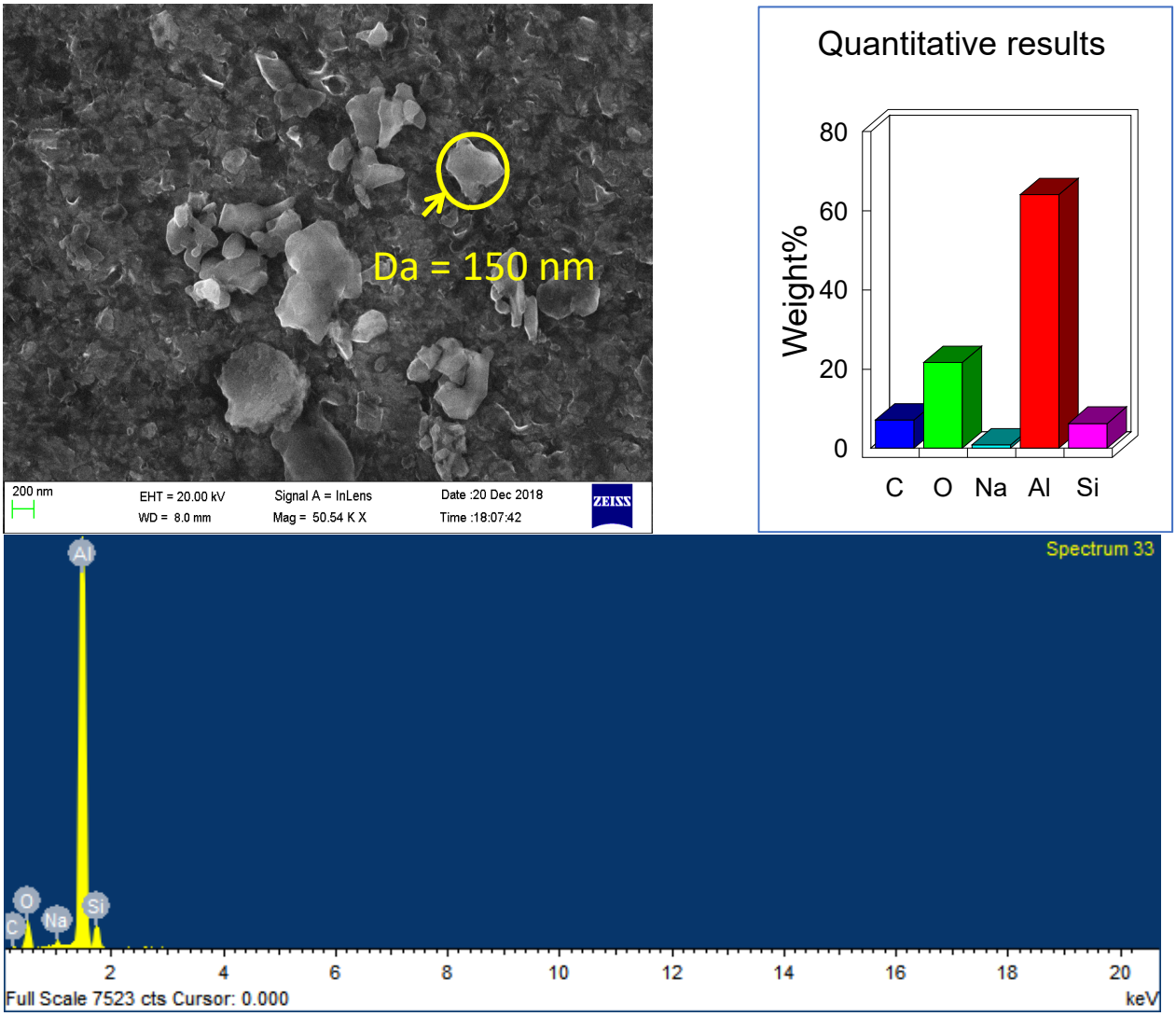

(**a**)

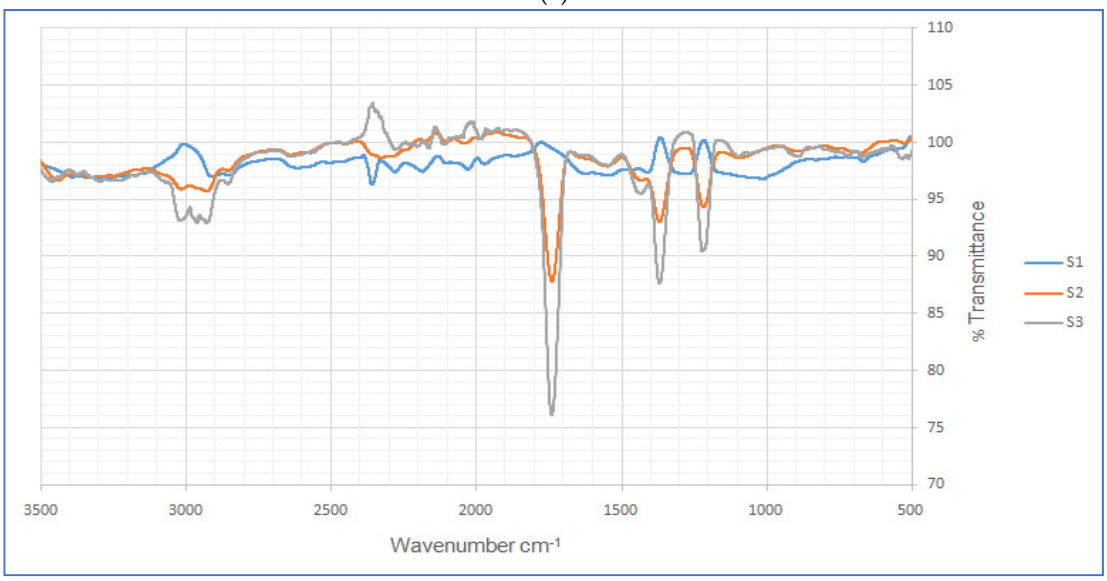

(**b**)

Figure 1. (**a**) SEM with EDX of nano-SiC reinforced aluminum matrix composites. (**b**) IR spectroscopy analysis of nano-SiC reinforced aluminum matrix composites.

Table 1. Details of aluminum and nano-SiC.

SL. NO.	Material	Size	Supplier	Purity
1	Aluminum	Billet	M/s Micro Fine chemicals, India	99.9%
2	Nano-SiC	50–80 nm	M/S US Research Nanomaterials Inc	99%

Table 2. Properties of lubricants used.

Properties	SAE20W40	Vegetable Oil (Cashew Nutshell Oil)	Vegetable Oil (Cashew Nutshell Oil + TiO_2)
Flash Point (°C) [ASTM D92]	200	214.27	190.2
Thermal Conductivity Watt/mK	0.152	0.161	0.169
Viscosity @100 °C (cSt) [ASTM D445]	15.2	15.48	16
Viscosity Index [ASTM D2270]	120	126	158

(**a**)

(**b**)

Figure 2. *Cont.*

(**c**)

Figure 2. (**a**) Four-ball wear test for SAE20W40. (**b**) Four-ball wear test for veg oil. (**c**) Four-ball wear test for veg oil + TiO_2.

2.2. Experimental Design

The experiments for this work are designed using an RSM-based Box–Behnken design and other designs to model and examine the responses to MQL-based grinding of composites. The design scheme is shown in Table 3. Based on the assessment, the number of experiments and the literature study analysis, five factors are changed over three levels.

Table 3. Grinding parameters and their levels.

Sl.No	Parameters	Notation	Unit	Levels		
				1	**2**	**3**
1	Wheel speed	*n*	rpm	900	1200	1500
2	Depth of cut	*d*	μm	10	20	30
3	Workpiece speed	*v*	rpm	80	150	270
4	wt % of nano-SiC	*w*	%	1	2	3
5	Type of MQL	-	-	SAE 20W40	VEG OIL	VEG OIL + TiO_2

2.3. Experimental Procedure

Experiments are carried out using an HMT-brand cylindrical machine with horizontal spindle (Type G13P). Aluminum oxide grinding wheel (AA60K5V8) is selected for grinding the MMNC cylindrical specimens. The MQL setup is attached as an alternative to the standard lubrication setup, and a flow rate of 50 mL/h is employed, which is controlled by the adjuster knob. The nozzle is placed between the grinding wheel and the workpiece interface at a distance of 35 mm. The details of the MQL system are presented in Figure 3.

A variable frequency drive (three-phase AC drive) is a type of motor controller, which drives an electric motor by varying the frequency and voltage supplied to the electric motor. The grinding wheel motor is coupled with a VFD setup, where the VFD exclusively runs it with run command and stops it with a stop command. If the VFD is coupled, then the complete control of input power will be exercised only by the VFD. The VFD has a range of 0–50 Hz, where 1 Hz reduces or increases 30 rpm. The maximum grinding wheel rpm is 1500. The complete circuit used for the present VFD is given in Figure 4. The following equation is used to determine the tangential grinding force (F_t) involved in this operation [8].

$$F_t = (P \times 94535)/V_s \quad (1)$$

where the tangential grinding force F_t is expressed in Newton, power P is expressed in kW, and wheel speed V_s is expressed in m/min. The workpiece surface temperature is recorded using a fluke-type infrared (Type 8839) thermometer allowing a measuring range of −50 to 1000 °C with an accuracy of ±2 °C. Before carrying out each experiment, the grinding wheel is dressed using a single-point diamond dresser. A surface roughness tester with a tip radius of 2 mm and evaluation and cut-off lengths of 4 mm and 0.8 mm, respectively, is employed for measuring the surface finish of the ground surface. The measurements are taken in the direction perpendicular to the cutting at six different points, and the average value of the readings is considered as the response. The experimental results are presented in Table 4. The schematic representation is presented in Figure 5.

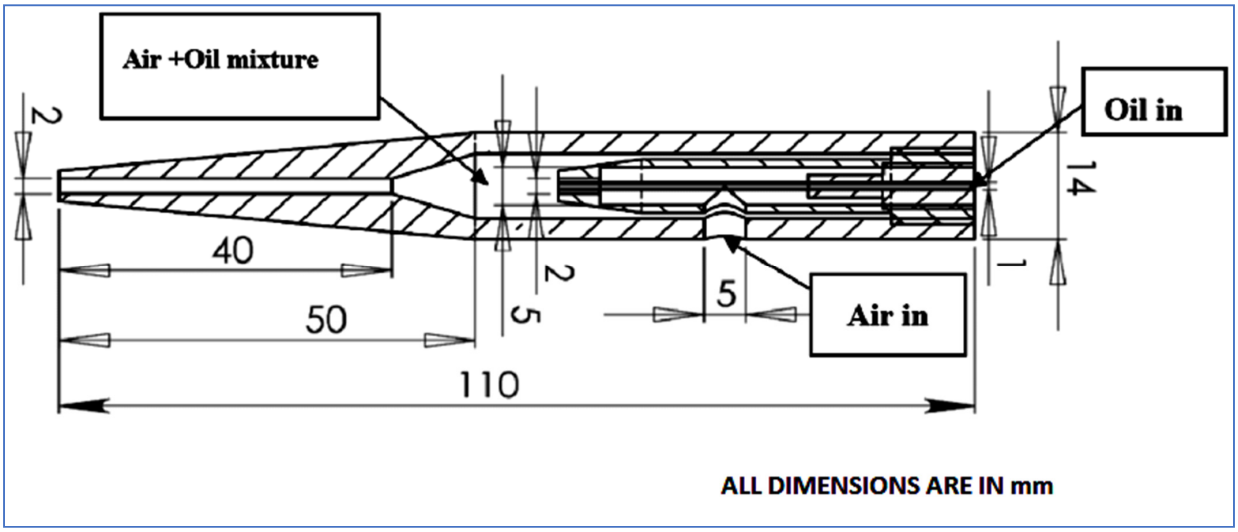

Figure 3. Details of MQL setup.

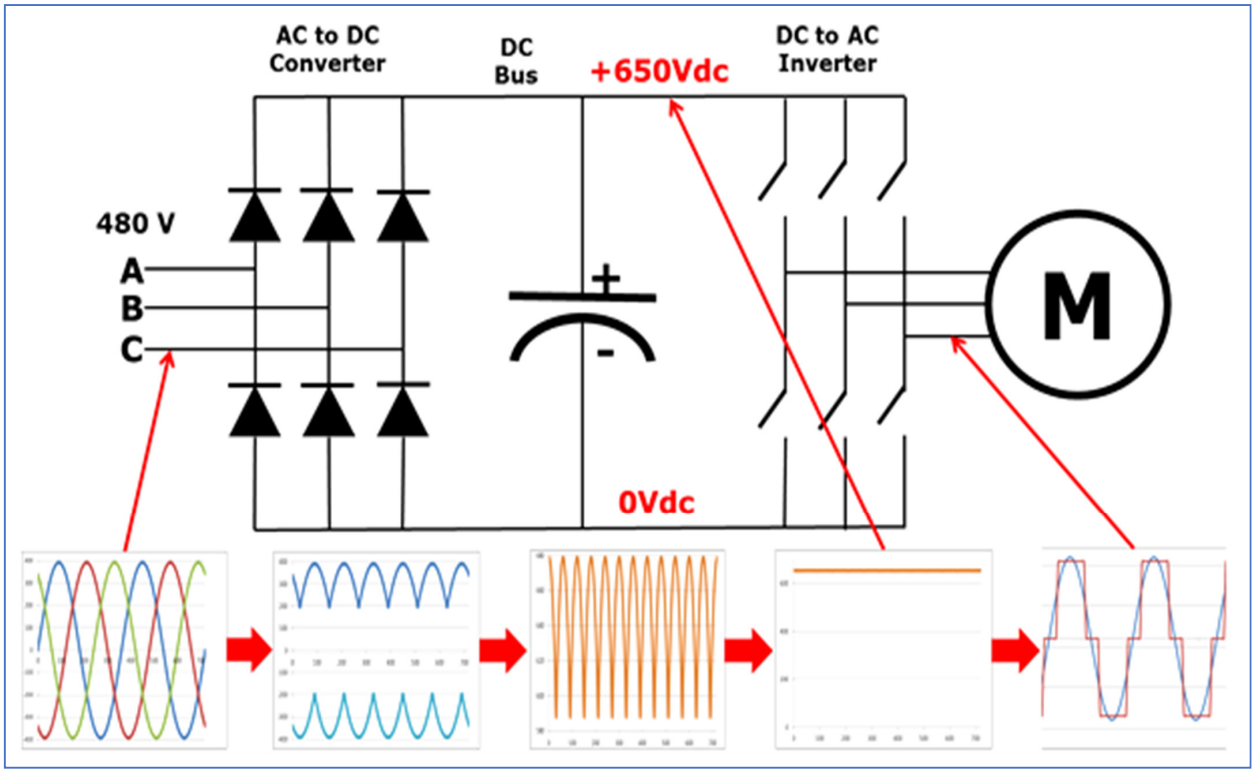

Figure 4. Circuit diagram of VFD setup.

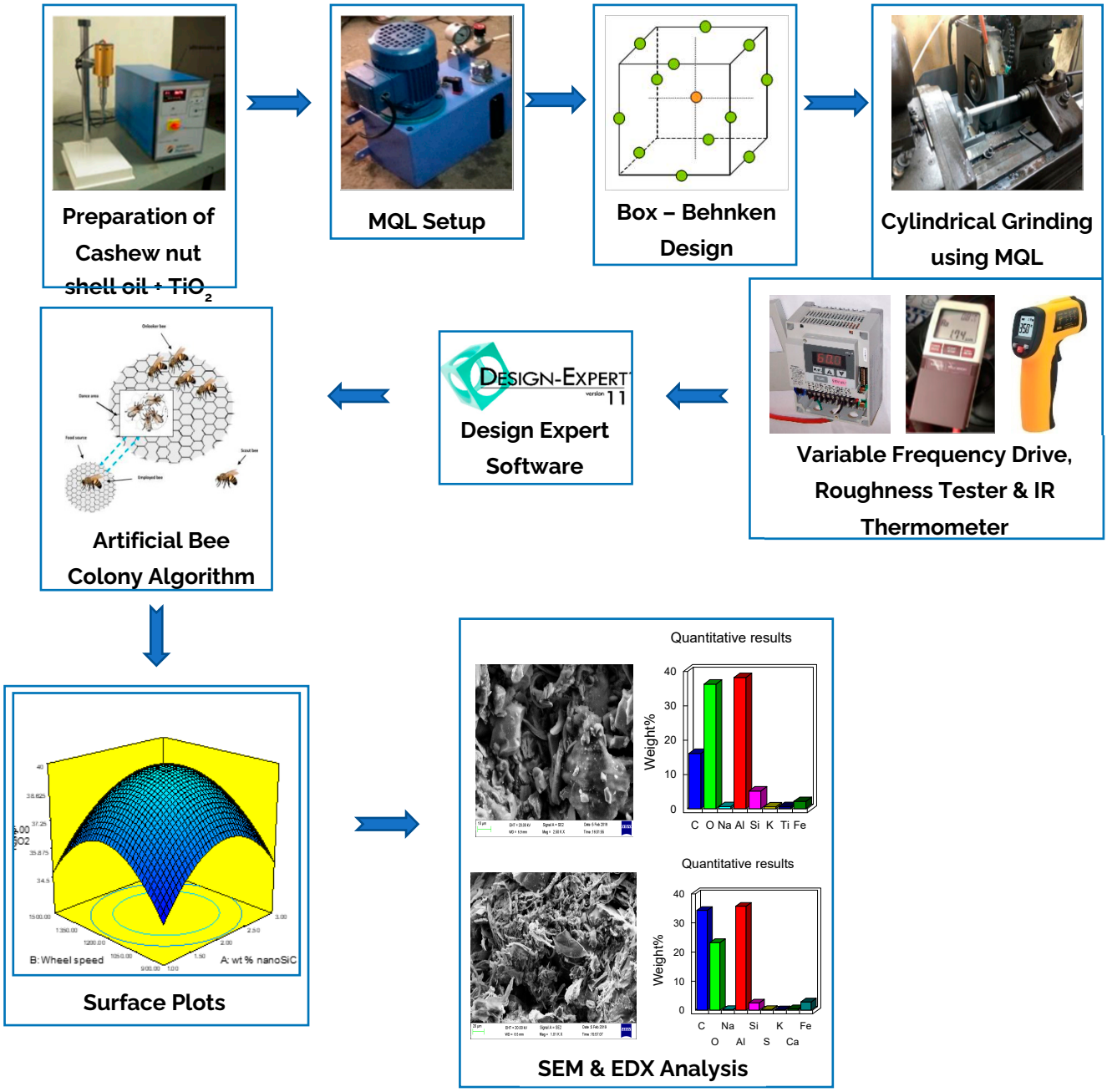

Figure 5. Schematic arrangement of experimental setup.

Table 4. Experimental results.

Sl. No	Weight %	Wheel Speed	Depth of Cut	Workpiece Speed	Surface Roughness			Temperature			Cutting Force		
					TiO_2	Veg Oil	SAE 20W40	TiO_2	Veg Oil	SAE 20W40	TiO_2	Veg Oil	SAE 20W40
1	1	900	20	175	2.01	2.060	1.911	43.30	44.382	45.492	52.54	53.853	55.199
2	3	900	20	175	1.45	1.486	1.223	34.85	35.721	36.614	53.38	54.714	56.082
3	1	1500	20	175	1.46	1.496	1.833	37.40	38.335	39.293	36.93	37.853	38.799
4	3	1500	20	175	1.12	1.148	2.117	36.60	37.515	38.452	35.07	35.946	36.845

Table 4. *Cont.*

Sl. No	Weight %	Wheel Speed	Depth of Cut	Workpiece Speed	Surface Roughness			Temperature			Cutting Force		
					TiO_2	Veg Oil	SAE 20W40	TiO_2	Veg Oil	SAE 20W40	TiO_2	Veg Oil	SAE 20W40
5	2	1200	10	80	1.74	1.783	1.828	55.60	56.990	58.414	54.38	55.739	56.133
6	2	1200	30	80	1.86	1.906	1.954	37.00	37.925	38.873	52.01	53.310	54.643
7	2	1200	10	270	1.58	1.619	1.659	36.82	37.740	38.684	52.64	53.956	55.304
8	2	1200	30	270	1.69	1.732	1.775	53.00	54.325	55.683	54.20	55.555	56.943
9	1	1200	20	80	2.50	2.562	2.626	46.69	47.857	49.053	52.17	53.474	54.811
10	3	1200	20	80	1.96	2.009	2.059	47.00	48.175	49.379	52.49	53.802	56.147
11	1	1200	20	270	2.01	2.060	2.111	52.00	53.300	54.632	54.12	55.473	56.998
12	3	1200	20	270	1.96	2.009	2.059	41.00	42.025	43.075	52.37	53.679	55.021
13	2	900	10	175	0.91	0.932	1.256	38.55	39.513	40.501	52.75	54.068	55.420
14	2	1500	10	175	1.09	1.117	1.145	36.40	37.310	38.242	35.08	35.957	37.855
15	2	900	30	175	0.94	0.963	0.987	36.78	37.699	38.642	52.80	54.120	55.473
16	2	1500	30	175	1.88	1.927	1.625	36.60	37.515	38.452	35.07	35.946	37.845
17	1	1200	10	175	2.50	2.562	2.226	42.71	43.777	44.872	53.00	54.325	55.683
18	3	1200	10	175	1.98	2.029	2.080	38.70	39.667	40.659	52.38	53.689	55.031
19	1	1200	30	175	2.28	2.337	2.395	43.00	44.075	45.176	53.17	54.499	55.861
20	3	1200	30	175	1.92	1.968	2.017	37.80	38.745	39.713	52.40	53.710	55.052
21	2	900	20	80	1.19	1.219	1.550	44.14	45.243	46.374	53.15	54.478	55.840
22	2	1500	20	80	1.12	1.148	1.176	43.35	44.433	45.544	36.00	36.900	37.822
23	2	900	20	270	0.69	0.707	0.724	43.50	44.587	45.702	55.79	57.184	55.691
24	2	1500	20	270	1.75	1.793	1.738	40.30	41.307	42.340	36.93	37.853	38.799
25	2	1200	20	175	2.20	2.255	2.321	41.80	42.845	43.946	52.17	53.474	54.836
26	2	1200	20	175	2.20	2.255	2.413	41.80	42.845	43.916	52.17	53.474	53.676
27	2	1200	20	175	2.20	2.255	2.391	41.80	42.845	43.927	52.17	53.474	54.795
28	2	1200	20	175	2.20	2.255	2.331	41.80	42.845	44.905	52.17	53.474	53.678
29	2	1200	20	175	2.20	2.255	2.381	41.80	42.845	43.916	52.17	53.474	54.811

3. Results and Discussion

3.1. Development of RSM-Based Design Models

The surface roughness, cutting force and temperature under MQL-based grinding of composites are examined through Box–Behnken design experimental models based on RSM. RSM is an association of statistical and mathematical techniques for modeling and analyzing uncertainties where the response is affected by restricted variables. Optimizing this response is the main objective of RSM [46].

The quadratic model for surface roughness is presented in Table 5, while Tables 6 and 7 correspond to the cutting force and temperature separately for various MQL approaches employing cashew nutshell oil+ Nano-TiO_2, cashew nutshell oil and SAE20W40. The values of β_o depend on the main grinding parameters, as well as investigational anomalies, such as surface finish, environmental conditions and machine vibrations. The experimental results and the β_o coefficient indicate that the MQL system based on cashew nutshell oil+ Nano-TiO_2 for reinforced composites performs better than other systems.

Table 5. Model for surface roughness.

Sl. No.	Type of MQL System	Model for Surface Roughness
1	SAE 20W40	$+2.36778 - 0.129083854 \times w + 0.165268625 \times n + 0.046581542 \times d - 0.093744271 \times v + 0.2430275 \times w \times n - 0.057975625 \times w \times d + 0.128701563 \times w \times v + 0.187117563 \times n \times d + 0.346799688 \times n \times v - 0.002626562 \times d \times v + 0.14542749 \times w^2 - 0.776037792 \times n^2 - 0.318537167 \times d^2 - 0.279312198 \times v^2$
2	Vegetable Oil (Cashew Nutshell Oil)	$2.255 - 0.20244 \times w + 0.105063 \times n + 0.065771 \times d - 0.05894 \times v + 0.056375 \times w \times n + 0.041 \times w \times d + 0.125563 \times w \times v + 0.19475 \times n \times d + 0.289563 \times n \times v - 0.00256 \times d \times v + 0.147771 \times w^2 - 0.81829 \times n^2 - 0.20842 \times d^2 - 0.24942 \times v^2$
3	Cashew Nutshell Oil + TiO_2	$2.2 - 0.1975 \times w + 0.1025 \times n + 0.064167 \times d - 0.0575 \times v + 0.055 \times w \times n + 0.04 \times w \times d + 0.1225 \times w \times v + 0.19 \times n \times d + 0.2825 \times n \times v - 0.0025 \times d \times v + 0.144167 \times w^2 - 0.79833 \times n^2 - 0.20333 \times d^2 - 0.24333 \times v^2$

Table 6. Model for cutting force.

Sl. No.	Type of MQL System	Model for Cutting Force
1	SAE 20W40	$54.35938 - 0.26438 \times w - 8.81162 \times n + 0.032553 \times d + 0.280113 \times v - 0.70917 \times w \times n - 0.0394 \times w \times d - 0.82824 \times w \times v - 0.01576 \times n \times d + 0.2816 \times n \times v + 0.782242 \times d \times v + 0.540918 \times w^2 - 8.19133 \times n\hat{}2 + 0.505257 \times d^2 + 0.868723 \times v^2$
2	Vegetable Oil (Cashew Nutshell Oil)	$53.47425 - 0.328 \times w - 8.99694 \times n - 0.04954 \times d + 0.499688 \times v - 0.69188 \times w \times n - 0.03844 \times w \times d - 0.53044 \times w \times v - 0.01537 \times n \times d - 0.43819 \times n \times v + 1.007063 \times d \times v + 0.136667 \times w^2 - 8.13124 \times n\hat{}2 + 0.118729 \times d\hat{}2 + 0.934885 \times v\hat{}2$
3	Cashew Nutshell Oil + TiO_2	$52.17 - 0.32 \times w - 8.7775 \times n - 0.04833 \times d + 0.4875 \times v - 0.675 \times w \times n - 0.0375 \times w \times d - 0.5175 \times w \times v - 0.015 \times n \times d - 0.4275 \times n \times v + 0.9825 \times d \times v + 0.133333 \times w^2 - 7.93292 \times n^2 + 0.115833 \times d^2 + 0.912083 \times v^2$

Table 7. Model for temperature.

Sl. No.	Type of MQL System	Model for Temperature
1	SAE 20W40	$44.12217 - 2.55214 \times w - 0.91667 \times n - 0.40274 \times d - 0.62687 \times v + 2.00932 \times w \times n - 0.31256 \times w \times d - 2.97064 \times w \times v + 0.517433 \times n \times d - 0.633 \times n \times v + 9.135184 \times d \times v - 0.17044 \times w^2 - 4.01572 \times n^2 - 1.23288 \times d^2 + 4.997327 \times v^2$
2	Vegetable Oil (Cashew Nutshell Oil)	$42.845 - 2.4899 \times w - 0.89431 \times n - 0.39292 \times d - 0.61158 \times v + 1.960313 \times w \times n - 0.30494 \times w \times d - 2.89819 \times w \times v + 0.504813 \times n \times d - 0.61756 \times n \times v + 8.912375 \times d \times v - 0.06577 \times w^2 - 3.81727 \times n^2 - 1.1023 \times d^2 + 4.975948 \times v^2$
3	Cashew Nutshell Oil + TiO_2	$41.8 - 2.42917 \times w - 0.8725 \times n - 0.38333 \times d - 0.59667 \times v + 1.9125 \times w \times n - 0.2975 \times w \times d - 2.8275 \times w \times v + 0.4925 \times n \times d - 0.6025 \times n \times v + 8.695 \times d \times v - 0.06417 \times w\hat{}2 - 3.72417 \times n^2 - 1.07542 \times d\hat{}2 + 4.854583 \times v^2$

The obtained experimental results are interpreted by applying the analysis of variance (ANOVA) at a significance level of $\alpha = 0.05$. The ANOVA results for surface roughness are presented in Table 8, while Tables 9 and 10 present the ANOVA results for the cutting force and temperature, respectively. A low probability value indicates that the models obtained may be considered statistically significant, which is desirable.

Table 8. ANOVA for surface roughness.

SAE20W40						
Source	**Sum of Squares**	**df**	**Mean Square**	**F-Value**	***p*-Value Prob > F**	
Model	6.562166	14	0.468726	136.9680487	<0.0001	significant
Residual	0.04791	14	0.003422			
Lack of Fit	0.041611	10	0.004161	2.642303478	0.1809	not significant
Pure Error	0.006299	4	0.001575			
Cor Total	6.610076	28				
Veg Oil						
Model	6.434834	14	0.459631	7.105710588	0.0004	significant
Residual	0.905586	14	0.064685			
Lack of Fit	0.905586	10	0.090559			
Pure Error	0	4	0			
Cor Total	7.34042	28				
Veg Oil + TiO_2						
Model	6.124767	14	0.437483	7.105711	0.0004	significant
Residual	0.86195	14	0.061568			
Lack of Fit	0.86195	10	0.086195			
Pure Error	0	4	0			
Cor Total	6.986717	28				

Table 9. ANOVA for cutting force.

SAE20W40						
Source	**Sum of Squares**	**df**	**Mean Square**	**F-Value**	***p*-Value Prob > F**	
Model	1450.225	14	103.5875	819.91239	<0.0001	significant
Residual	1.768756	14	0.12634			
Lack of Fit	0.2169	10	0.02169	0.0559074	0.9999	not significant
Pure Error	1.551855	4	0.387964			
Cor Total	1451.993	28				
Veg Oil						
Model	1473.202	14	105.2287	322.9143	<0.0001	significant
Residual	4.562208	14	0.325872			
Lack of Fit	4.562208	10	0.456221			
Pure Error	0	4	0			
Cor Total	1477.764	28				
Veg Oil + TiO_2						
Model	1402.215	14	100.1582	322.914327	<0.0001	significant
Residual	4.342375	14	0.31017			
Lack of Fit	4.342375	10	0.434238			
Pure Error	0	4	0			
Cor Total	1406.557	28				

Table 10. ANOVA for temperature.

SAE20W40						
Source	**Sum of Squares**	**df**	**Mean Square**	**F-Value**	***p*-Value Prob > F**	
Model	824.2409	14	58.87434862	226.0325839	<0.0001	significant
Residual	3.646558	14	0.260468414			
Lack of Fit	2.879526	10	0.287952589	1.501645942	0.3700	not significant
Pure Error	0.767032	4	0.191757977			
Cor Total	827.8874	28				
Veg Oil						
Model	784.3493	14	56.02495	286.1780157	<0.0001	significant
Residual	2.740774	14	0.19577			
Lack of Fit	2.740774	10	0.274077			
Pure Error	0	4	0			
Cor Total	787.0901	28				
Veg Oil + TiO_2						
Model	746.555	14	53.32536	286.178	<0.0001	significant
Residual	2.608708	14	0.186336			
Lack of Fit	2.608708	10	0.260871			
Pure Error	0	4	0			
Cor Total	749.1637	28				

3.2. Multi-Objective Optimization Using the Artificial Bee Colony (ABC) Algorithm

Artificial bee colony (ABC) algorithm is a metaheuristic algorithm established in 2005 by Karaboga and Basturk [32], mimicking the natural foraging behavior of honey bee swarms. Compared to other evolutionary algorithms, such as harmony search, differential evolution, particle swarm algorithm, genetic algorithm and simulated annealing algorithm, ABC algorithms have the advantages of fewer parameters, simpler structure and simpler implementation in any complex task [9,33]. The employed bees are mainly responsible for looking at the food sources, as well as sharing the information on food resources with onlooker bees. If the number of food sources cannot be improved over the number of trials, the employed bees and onlooker bees become a scout bee, which generates a new random food source. In the last step in the cycle, when bees abandon the nectar food source, a new food source is randomly allocated to a scout bee and changed with the earlier one. Further, the above three steps are repeated by a programed number of cycles until the program reaches the final criteria. The food source is selected by an artificial observer bee based on the probability related to the food source (Pi), which is calculated by Equation (1):

$$P_i = \frac{f_i t_i}{\sum_{n=1}^{SN} f_i t_n} \quad (2)$$

where $f_i t_i$ represents the exact quantity of solution i, which is relative to the quantity of the food source nectar in location i, and SN is the number of food sources relative to the sum of the observer or employed bees. A candidate food location is generated in the process from the old one in the memory using Equation (2).

$$v_{ij} = x_{ij} + \Phi_{ij}\left(x_{ij} - x_{kj}\right) \quad (3)$$

where $k \in 1, 2, \ldots$ SN and $j \in 1, 2, \ldots$ D are randomly selected items. Φ_{ij} is a random number in a range from -1 to 1, which governs food source creation regarding X_{ij} and

evaluates two food locations based on a reducing food source of X_{ij}. The new food source discovered by the scout bees replaces the nectar providing the present food source.

If the abandoned source is assumed as x_i and $j \in \{1,2, \ldots .D\}$, the new food source discovered by the scout bees will replace x_i. Equation (3) calculates the bees performance.

$$x_i^j = x_{min}^j + \text{rand}[0, 1]\left(x_{max}^j - x_{min}^j\right) \quad (4)$$

After creating the V_{ij} position for every candidate food source, the artificial bee evaluates it and then compares the performance with the former one. If the nectar of the new food source is better when compared with the previous one, then the new food source will replace the old one.

In a multi-objective optimization, instead of treating the responses individually, all the responses are optimized simultaneously [35]. However, both single-objective optimization and multiple-objective optimization are carried out in order to develop multi-objective function (MOF). The multi-objective optimization model is formulated for demonstrating and validating the multi-objective ABC algorithm to optimize the grinding process parameters as follows.

Objective 1: Minimization of surface roughness

$$\begin{aligned}\text{Surface roughness} = {} & -6.41215 - 1.52907 \times w + 0.017042 \times n + 0.065639 \times d - 7.76648 \times 10^{-3} \times v + 6.26783 \times 10^{-4} \\ & \times w \times n - 5.79756 \times 10^{-3} \times w \times d + 1.35475 \times 10^{-3} \times w \times v + 6.23725 \times 10^{5} \times n \times d + 1.21684 \times 10^{-5} \times n \times v - \\ & 2.76480 \times 10^{-6} \times d \times n + 0.12710 \times w^2 - 8.82632 \times 10^{-6} \times n^2 - 3.09372 \times 10^{3} \times d^2 - 2.99332 \times 10^{-5} \times v^2\end{aligned} \quad (5)$$

Objective 2: Minimization of temperature

$$\begin{aligned}\text{Temperature} = {} & +38.95727 - 3.81033 \times w + 0.091072 \times n - 1.37438 \times d - 0.30353 \times v + 6.69773 \times 10^{-3} \times w \times n - \\ & 0.031256 \times w \times d - 0.031270 \times w \times v + 1.72478 \times 10^{-4} \times n \times d - 2.22106 \times 10^{-5} \times n \times v + 9.61598 \times 10^{-3} \times d \times v - \\ & 0.17044 \times w^2 - 4.46191 \times 10^{-5} \times n^2 - 0.012329 \times d^2 + 5.53720 \times 10^{-4} \times v^2\end{aligned} \quad (6)$$

Objective 3: Minimization of cutting force

$$\begin{aligned}\text{Cutting force} = {} & -45.44908 + 3.00705 \times w + 0.19920 \times n - 0.21707 \times d - 0.028194 \times v - 2.36391 \times 10^{-3} \times w \times n - \\ & 3.93984 \times 10^{-3} \times w \times d - 0.011355 \times w \times v - 5.25260 \times 10^{-6} \times n \times d + 8.12632 \times 10^{-6} \times n \times v + 8.23413 \times 10^{-4} \times d \\ & \times n + 0.38692 \times w^2 - 9.38397 \times 10^{-5} \times n^2 + 2.26018 \times 10^{-3} \times d^2 + 8.19636 \times 10^{-5} \times v^2\end{aligned} \quad (7)$$

Based on the above objective considerations, the following multi-objective function is developed, and it is presented in Equation (4):

$$\text{Min}(z_1) = w_1 Y_u(\text{SR})/\text{SR}_{min} + w_2 Y_u(\text{Temp})/\text{Temp}_{min} + w_3 Y_u(\text{CF})/\text{CF}_{min} \quad (8)$$

where Y_u(SR), Y_u(Temp) and Y_u(CF) are the quadratic responses of the second order, as represented by the equation. SR_{min}, Temp_{min} and CF_{min} are the minimum values obtained from single-objective optimization using the ABC algorithm. w_1, w_2 and w_3 are the weight values of each response. Weight values for anything can be provided; however, usually, this can be set by the process engineer depending on the significance of each response and must be equal to $w_1 + w_2 + w_3 = 1$. Therefore, according to the present investigation, $w_1 = w_2 = w_3 = 0.333$. The mathematical model developed based on the multi-objective function is

$$\begin{aligned}\text{MOO} = {} & -1.679158412 - 0.548057133 \times x(1) + 0.007340723 \times x(2) + 0.004611971 \times x(3) - 0.005384516 \times x(4) + \\ & 0.000279656 \times x(1) \times x(2) - 0.002031593 \times x(1) \times x(3) + 2.8599 \times 10^{-5} \times x(1) \times x(4) + 1.99025 \times 10^{-5}\, x(2) \times x(3) + \\ & 3.45841 \times 10^{-6} \times x(3) \times x(4) + 9.63241 \times 10^{-5}\, x(3) \times x(4) + 0.04598869 \times x(1)^2 - 3.76321 \times 10^{-6} \times x(2)^2 - \\ & 0.001006651 \times x(3)^2 - 3.07065 \times 10^{-6} \times x(4)^2\end{aligned} \quad (9)$$

The computer code is developed for the ABC algorithm using MATLAB with the following controlling factors chosen for obtaining the smooth parametric optimization problem convergence. The ABC algorithm controlling parameters are as follows:

Number of scout bees: 1,

Number of onlooker bees: 50,
Number of food sources: 25,
Number of iterations: 100.

The results obtained from the ABC algorithm are compared to the previous research works to confirm the adequacy of the results. The results obtained using the ABC algorithm are presented in Table 11, and the iteration chart is presented in Figure 6. The optimized result shows that the nano-filled MQL could significantly reduce grinding forces and enhance surface quality. Nano-fluid-exposed grinding showed improved tribological and thermophysical properties and reduced the cutting forces and surface roughness, cutting zone temperature and tool wear [5].

Table 11. Multi-objective optimization results for grinding process.

Parameters and Objective Function	Value		
	TiO_2	**Veg Oil**	**SAE20W40**
Percentage of weight		2.9024	
Wheel speed rpm		910.0719	
Depth of cut µm		29.4243	
Workpiece speed rpm		78.6531	
Surface roughness µm	1.01134	1.1014	1.15263
Temperature in deg c	34.1609	35.5801	34.83
Cutting force in N	36.2115	37.1424	37.1465
Multi-objective function (Z_1)		0.99145	

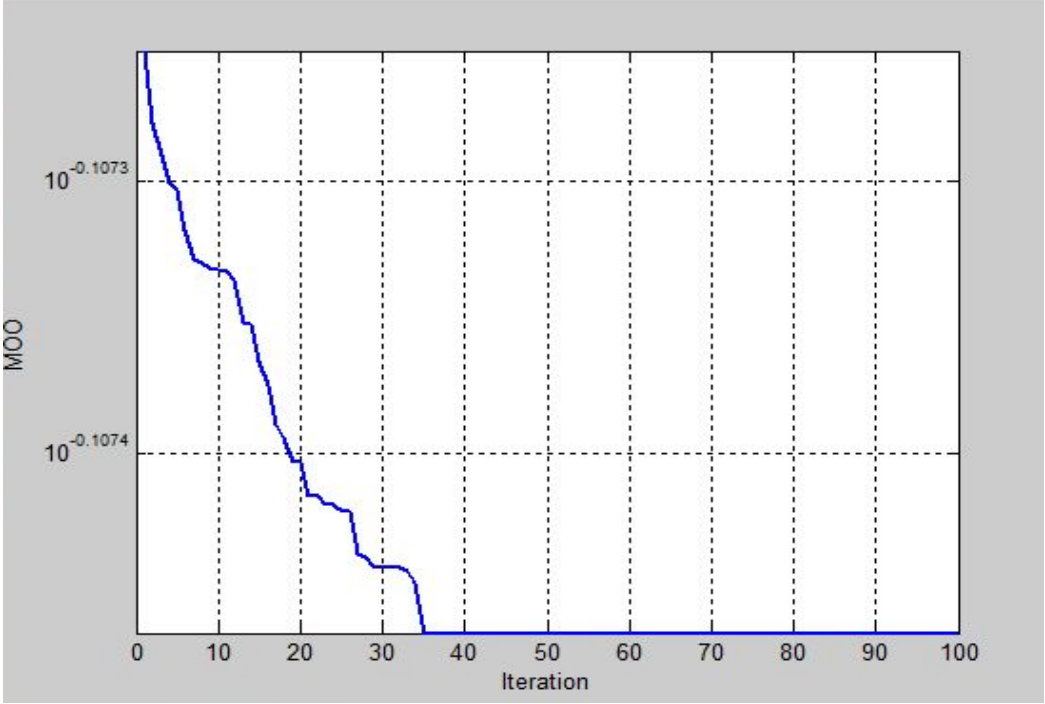

Figure 6. Iteration chart using ABC algorithm.

3.3. Influence of Grinding Parameters on Responses

The 3D surface plots of models fitted for surface roughness on grinding parameters are shown in Figure 7. The wheel velocity is found to be a prominent influencing factor that affects surface roughness. The increase in wheel velocity reduces the chip thickness, justifying the prominent wheel velocity effect on surface roughness [47]. The ground surface quality of aluminum composites is influenced by the reinforcement particles. In all

grinding conditions, the surface roughness decreases as the wt % of nano-SiC increases. The hardness, heat resistance and tensile strength were increased by the addition of nano-SiC in an Al matrix [48]. The experimental result shows the reduction in surface roughness as the wt % of nano-SiC increases. Suna et al. established that surface roughness increases with an increase in the depth of cut. When the depth of cut is increased, the increase in material removal rate and the increase in chip thickness account for the increase in surface roughness values [49]. Thiyagarajan et al. found that surface roughness decreases with an increase in wheel velocity and workpiece velocity. This is due to the increase in relative velocity between the wheel and the workpiece and the reduction in contact time, thereby reducing chip thickness[17]. Tawakoli et al. discussed that increasing the depth of cut and the wheel speed leads to an increase in the penetration of each grain in the workpiece in the contact zone, lower amounts of uncut chips left on the ground surface, and consequently, lower surface roughness can be observed in MQL grinding compared to dry grinding.

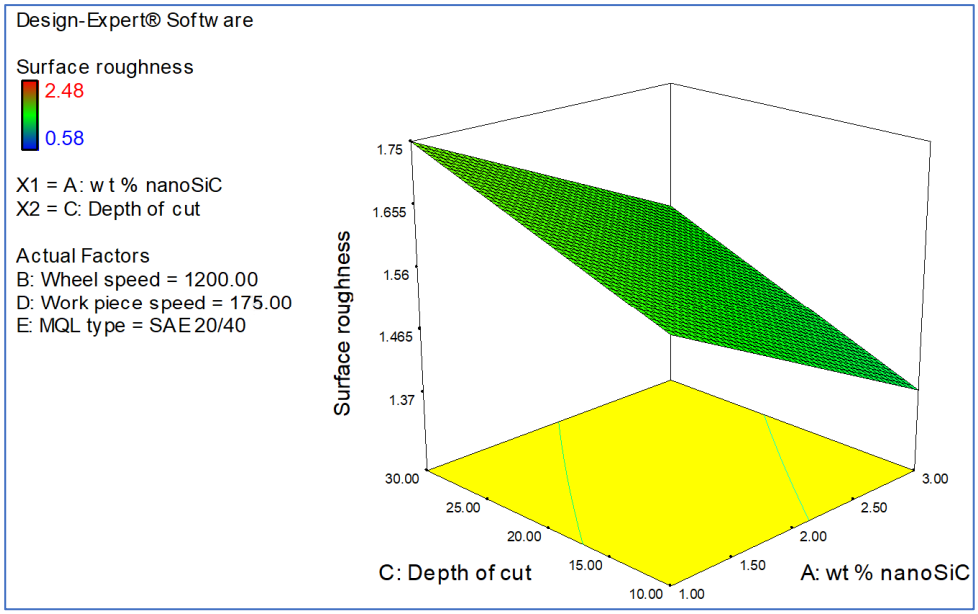

(**a**)

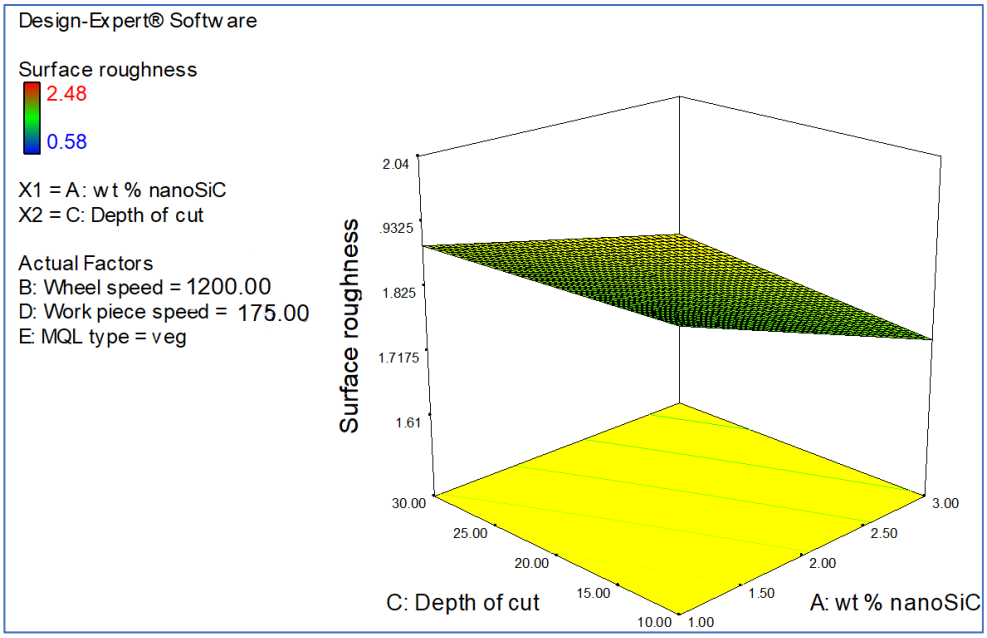

(**b**)

Figure 7. *Cont.*

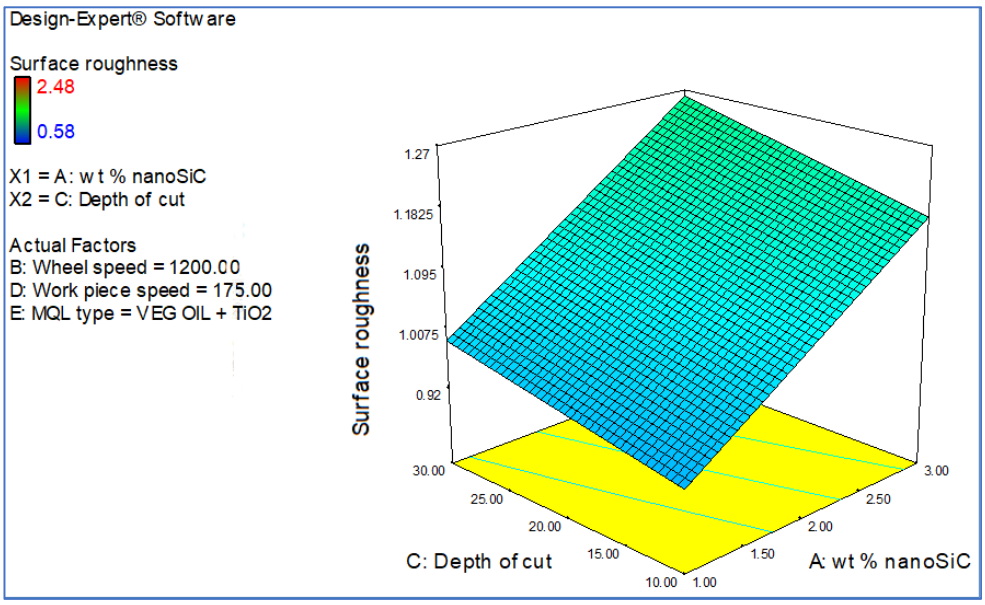

(**c**)

Figure 7. (**a**) 3D response plot for SR on wt % of nano-SiC vs. depth of cut under SAE20W40. (**b**) 3D response plot for SR on wt % of nano-SiC vs. depth of cut under veg oil. (**c**) 3D response plot for SR on wt % of nano-SiC vs. depth of cut under veg oil + TiO_2.

The experiments indicated a reduction in surface roughness with an increase in wt % of nano-SiC. The hardness of the composites greatly affects surface roughness and thereby improves MMNC grinding surface finish [30].

Figure 8 presents the 3D surface plots of models fitted for the cutting force on grinding factors. One of the most important parameters is the tool life, which regularly decreases as the cutting force and depth of cut increase owing to increased stress and contact of the workpiece. More cutting force is generated with rapid tool advancement and vibrations resulting in an increase in surface roughness Surface roughness is increased as a result of high cutting force, which is generated through vibrations and rapid tool movement [50] The experiments point out that the tangential force is decreased when the wheel speed and workpiece speed are increased. When the depth of cut increases, the tangential grinding force and surface roughness are increased. The MQL system based on cashew nutshell oil+ Nano-TiO_2 attained the best performance, as the MQL system lubricant infiltrates the wheel and the workpiece boundary contact region [51]. Thiyagarajan et al. concluded that the tangential grinding force decreases with an increase in wheel velocity and workpiece velocity. This could be attributed to the thermally induced softened matrix at high speeds. As the grinding wheel velocity increases, the heat generated in the deformation zone increases, thereby softening the aluminum matrix, thus reducing the force required to remove the material [17]. Cong Mao et al. found that MQL grinding has a lower grinding force in comparison with dry grinding. This demonstrates that the MQL system can penetrate the contact zone between the workpiece and the wheel to lubricate the contact zone [32]. Dinesh et al. found that the grinding forces in the case of nano-fluid MQLs decreased effectively in both normal and tangential directions. It is observed from the experiments that the increase in workpiece speed and wheel speed resulted in a decrease in the tangential grinding force, while the increase in depth of cut increased the tangential grinding force and surface roughness. The force reduction in the grinding processes could be attributed to the enhanced lubrication and cooling characteristics of the nano-cutting fluid [27].

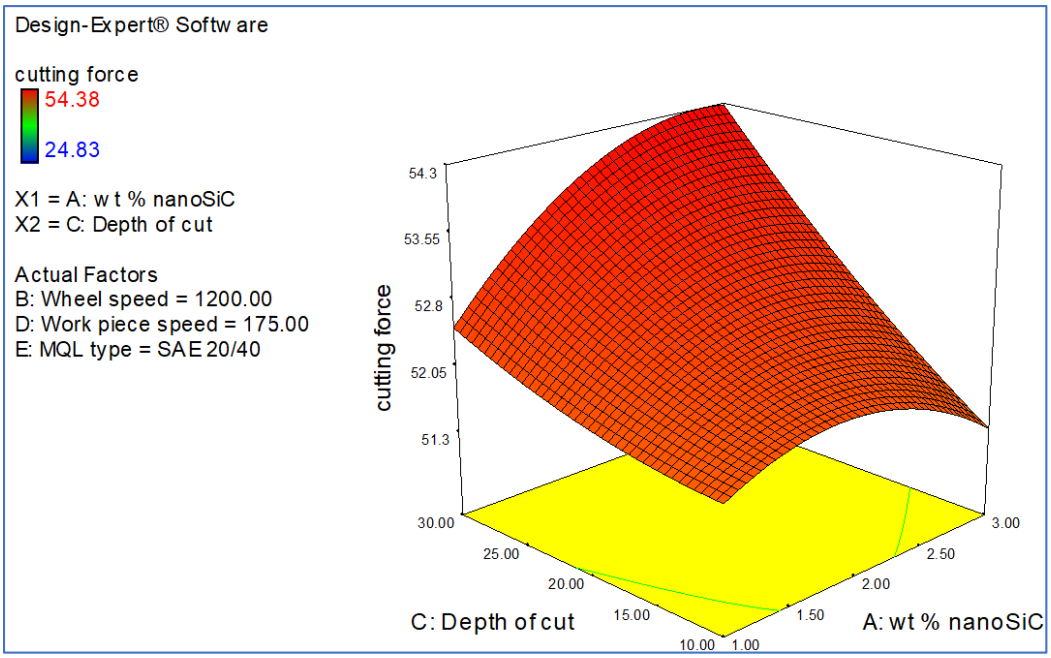

(**a**)

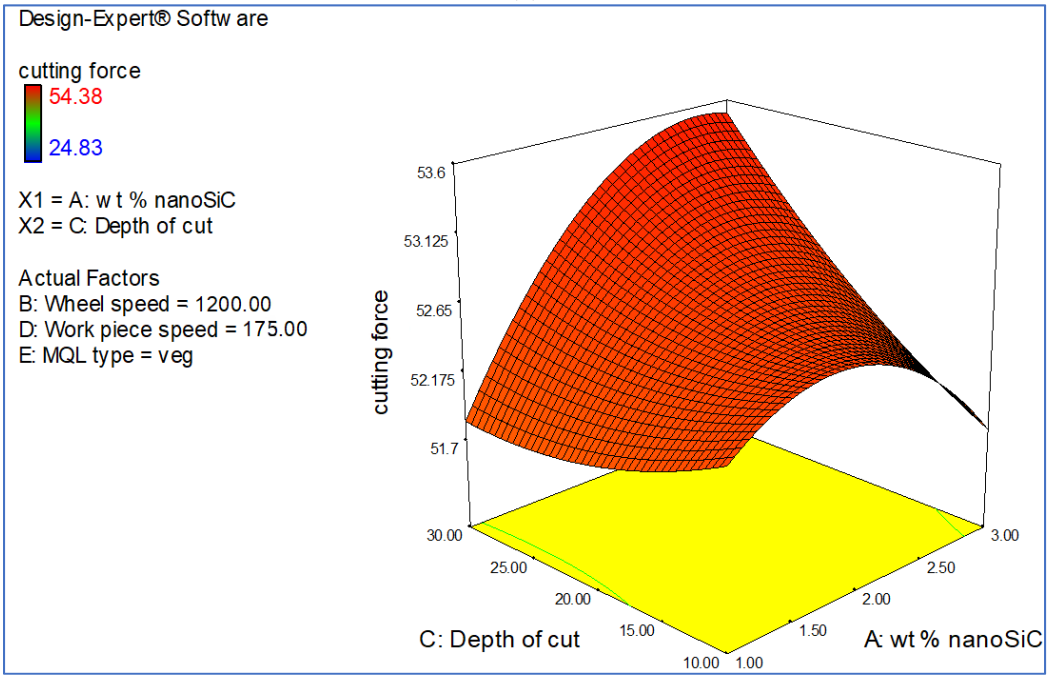

(**b**)

Figure 8. *Cont.*

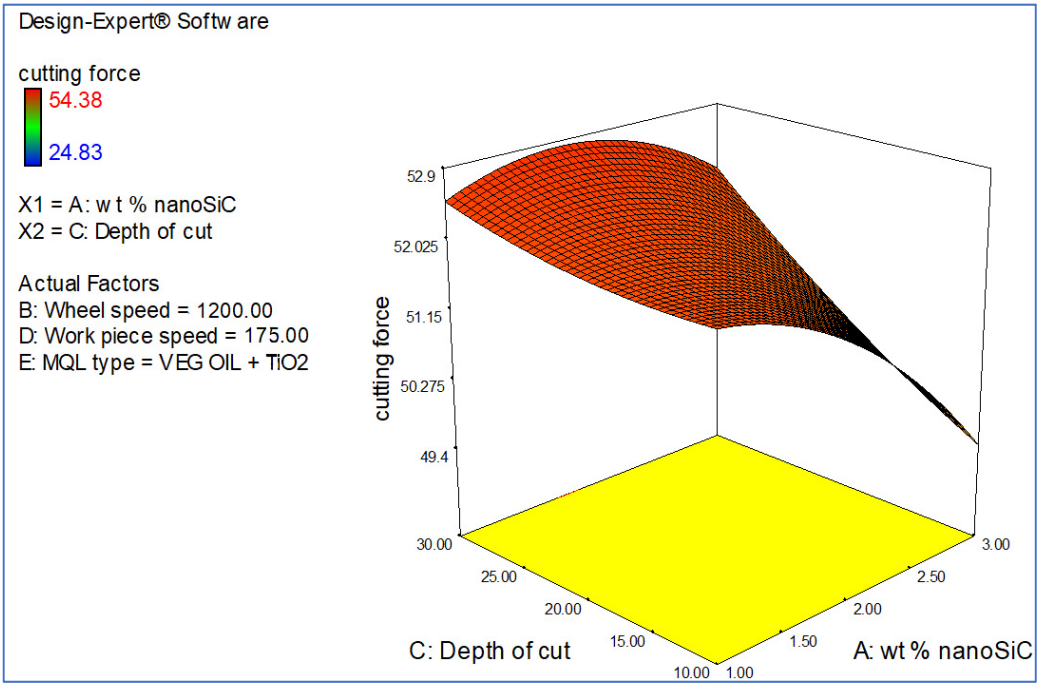

(**c**)

Figure 8. (**a**) 3D response plot for CF on wt % of nano-SiC vs. depth of cut under SAE20W40. (**b**) 3D response plot for CF on wt % of nano-SiC vs. depth of cut under veg oil. (**c**) 3D response plot for CF on wt % of nano-SiC vs. depth of cut under veg oil + TiO_2.

Three-dimensional surface plots of models fitted for the temperature on grinding parameters are shown in Figure 9. The heat resistance, hardness and tensile strength are influenced by the addition of nano-SiC in the Al matrix; the temperature decreases with the increase in wt % of nano-SiC [52] The MQL grinding process is compared with dry grinding results, the benefits of reducing the grinding forces, improving surface roughness and preventing the workpiece from burning. MQL grinding could remarkably lower the grinding temperature [53]. It is evident from the experimental results that the grinding temperature is decreased with the increase in wt % of nano-SiC particles. The lubricant filled with nano-particles plays a vital role in the actual grinding process by carrying heat throughout the process, thereby improving the surface finish. Thiyagarajan et al. found that the grinding temperature increases with an increase in wheel velocity, workpiece velocity and depth of cut. The higher values of wheel velocity, workpiece velocity and depth of cut result in higher grinding temperature due to the increase in the energy required to grind a unit volume of the metal [17].

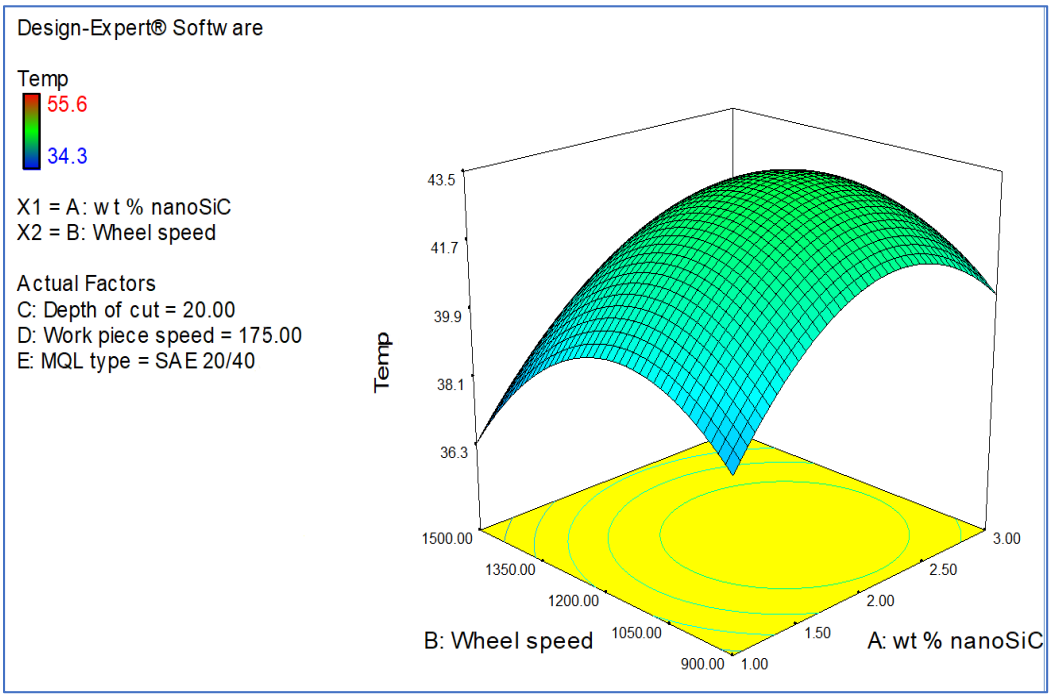

(**a**)

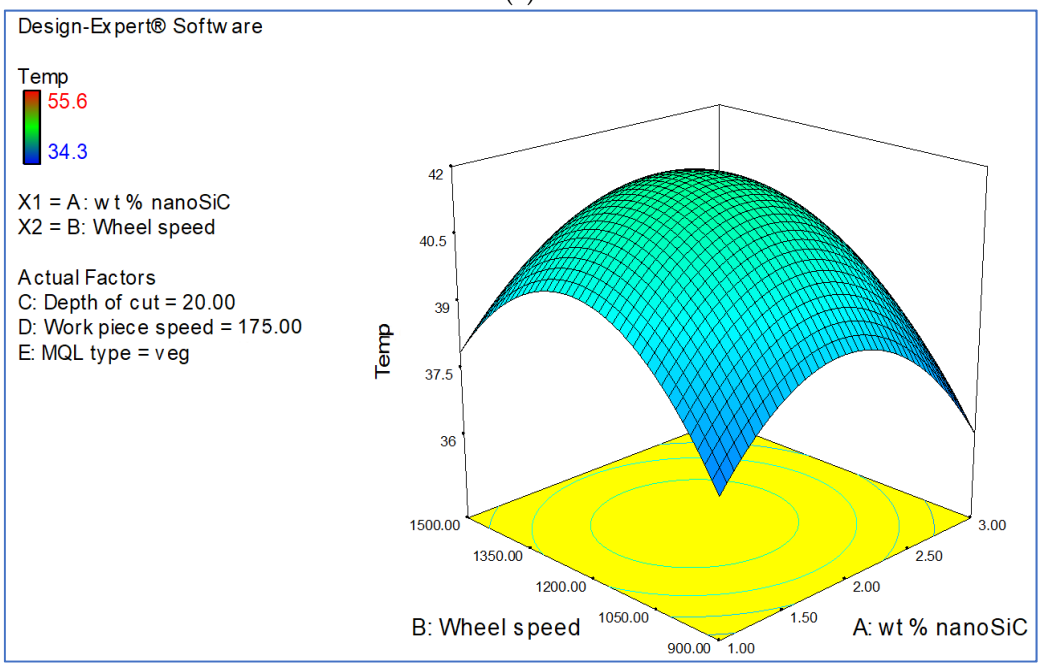

(**b**)

Figure 9. *Cont.*

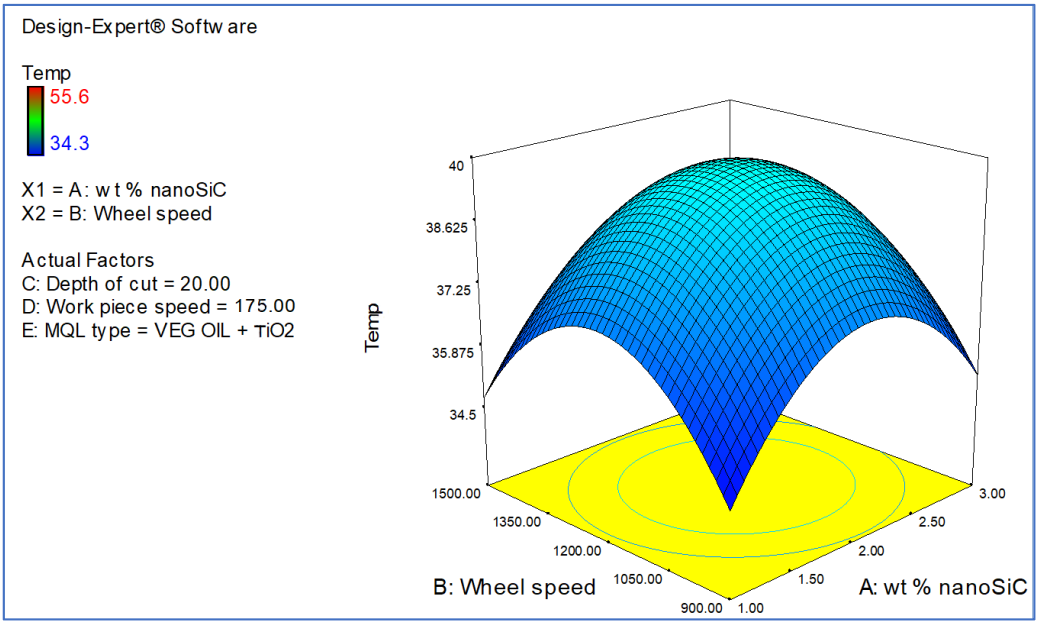

(**c**)

Figure 9. (**a**) 3D response plot for TEMP on wt % of nano-SiC vs. wheel speeds under SAE20W40. (**b**) 3D response plot for TEMP on wt % of nano-SiC vs. wheel speed under veg oil. (**c**) 3D response plot for TEMP on wt % of nano-SiC vs. wheel speed under veg oil + TiO_2.

Cong Mao et al. found that the temperature in dry grinding is considerably higher than that in MQL grinding. The best performance obtained by cashew nutshell oil+ Nano-TiO_2 based MQL is mainly due to the lubricity of the utilized fluid and the decrease in grinding temperature. This indicates that the heat-collecting ability of the nano-fluid is increased. This is due to the lack of lubrication and cooling for dry grinding [54]. Cong Mao et al. found that the grinding temperature decreases with an increase in air pressure, which enhances the nano-fluid mist in penetrating the grinding zone [32]. Thiyagarajan et al. found that the grinding temperature increases with an increase in wheel velocity, workpiece velocity and depth of cut. The higher values of wheel velocity, workpiece velocity and depth of cut result in higher grinding temperature due to the increase in the energy required to grind a unit volume of the metal [17].

3.4. Surface Morphology of the Machined Surface

Scanning electron microscopy (SEM) was employed for observing and analyzing the machined surface morphologies. Figure 10 presents the micro-graphs obtained through SEM. The increased depth of cut and cutting force resulted in the fragmentation of Al_2O_3 grains of the grinding wheel and implantation on the workpiece surface. The workpiece under SAE20W40 lubrication exhibits grinding wheel marks on the surface and poor surface finish, which is attributed to the high depth of cut. The grinding wheel material plunges into the workpiece surface as a result of the increased depth of cut [55]. Zhu et al. found that the interface strength and interior cracks of silicon carbide are the causes of cavity defects [56]. Guoqiang et al. proved that surface topography is related to the feeding velocity and grinding depth (the higher the feeding velocity and grinding depth, the more uneven the surface topography), and the impact caused by the feeding velocity is more significant than that caused by the grinding depth [14]. It is distinctly clear from the micro-graph that the surface finish is excellent under MQL based on cashew nutshell oil + Nano-TiO_2. Micro-cracks are formed on the machined surface due to the difference in thermal expansion between the nano-SiC particles and Al.

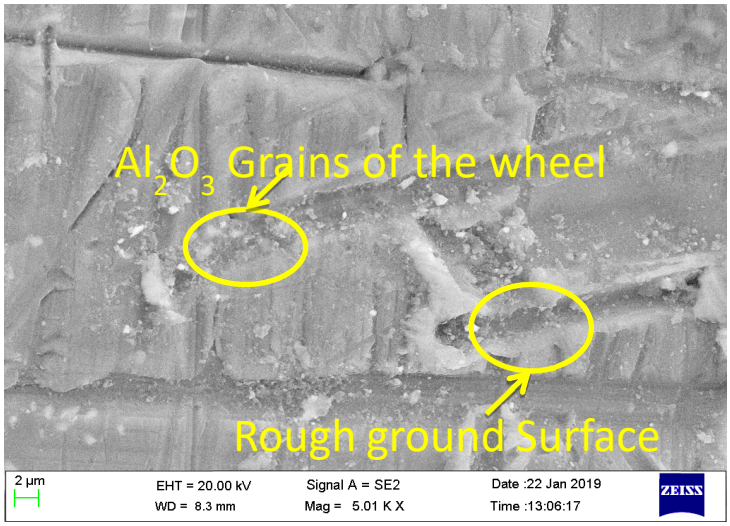

(**a**)

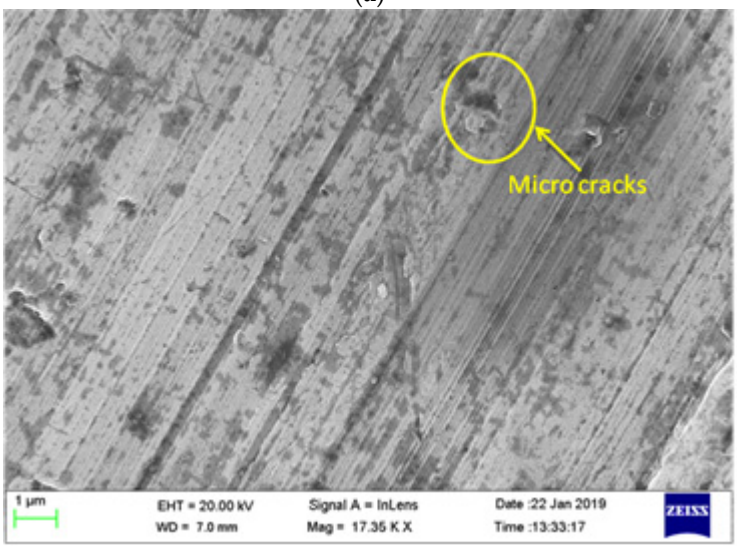

(**b**)

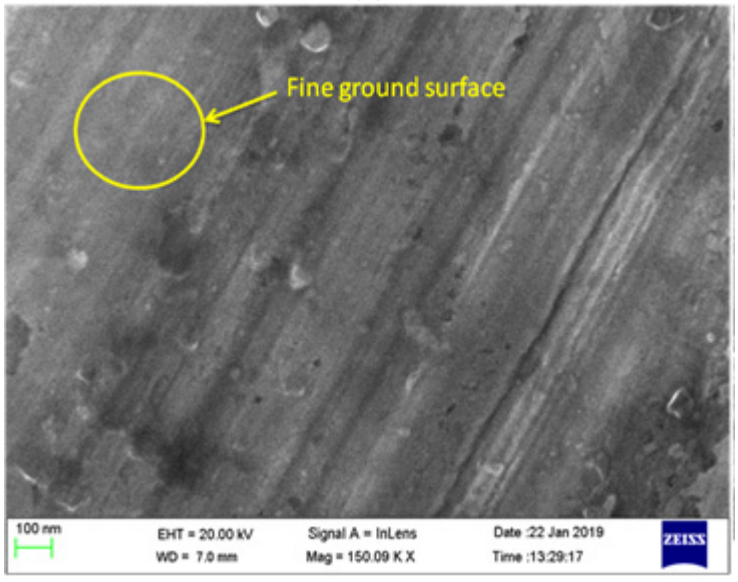

(**c**)

Figure 10. (**a**) Micro-structure of machined surface under SAE20W40. (**b**) Micro-structure of machined surface under veg oil. (**c**) Micro-structure of machined surface under veg oil + TiO_2.

3.5. Surface Morphology of Grinding Wheel

The grinding wheel is examined using SEM under different MQL systems, which are presented in Figure 11. The grinding wheel contains capillary networks or holes, which act as micro-reservoirs to store the nano-fluids temporarily [57]. The TiO_2 nano-particles are carried into the grinding zone by these micro-reservoirs; in addition, a vast volume of nano-fluids can be delivered by high-porosity grinding wheels. A lubricating film layer of the TiO_2 nano-fluid can be formed on the abrasive grain surfaces through chemical and physical reactions of nano-fluids. The wear flattening generation is prevented and effectively forced to drop from the abrasive grains by this layer. Adibi et al. found that dry grinding has the highest value of wear flattening area, resulting in rapid blunting of abrasive grains and high amounts of grinding forces [28]. Nevertheless, the wear flattening areas on the wheel's surface after MQL grinding and fluid grinding are roughly similar to each other.

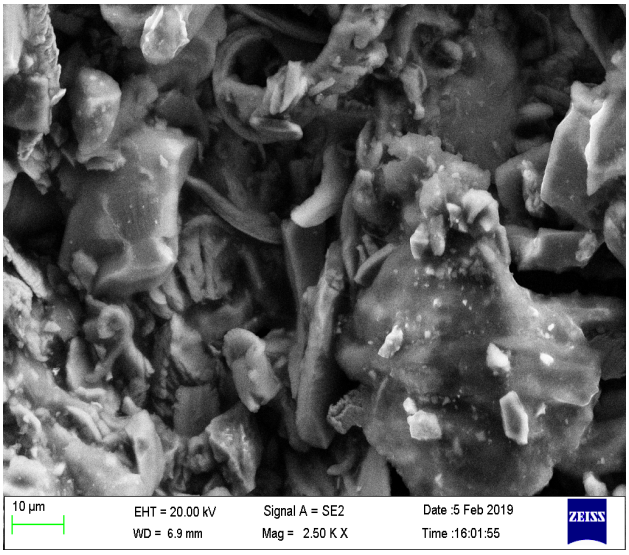

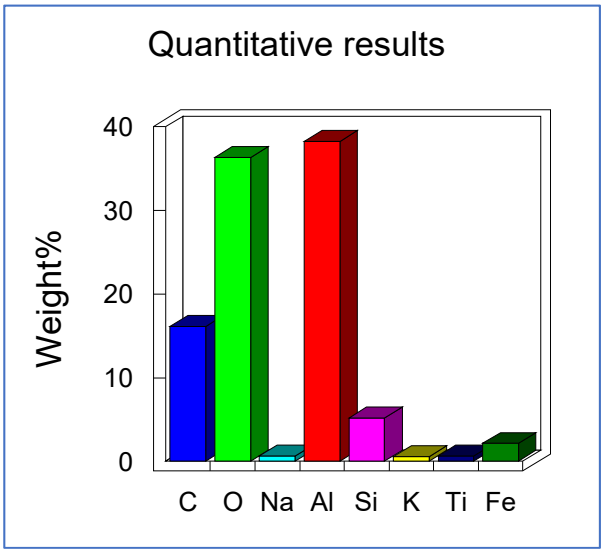

(**a**)

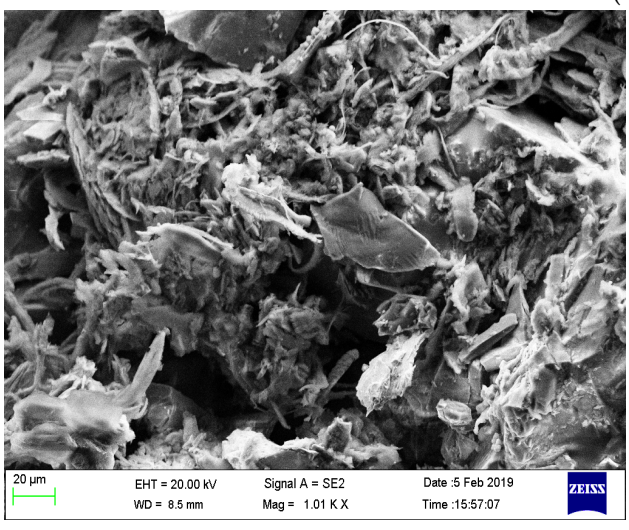

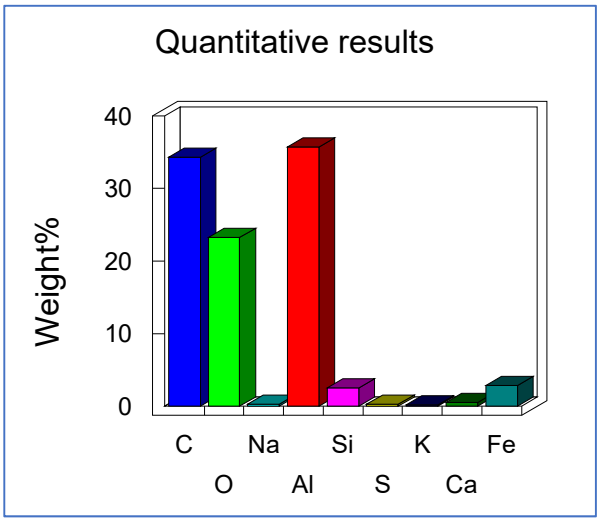

(**b**)

Figure 11. *Cont.*

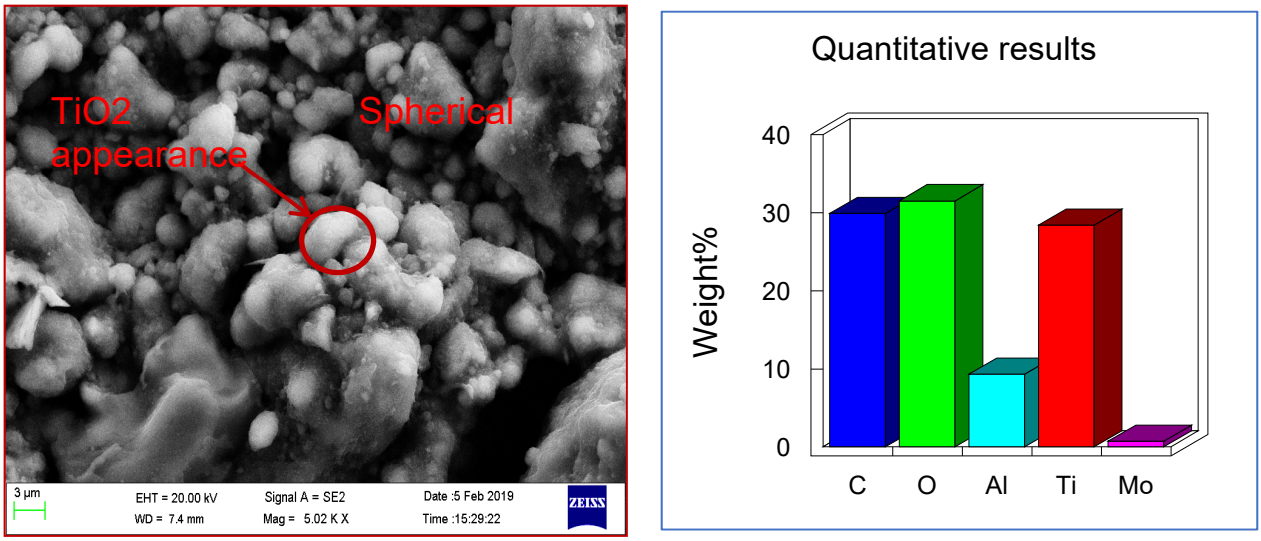

(**c**)

Figure 11. (**a**) Micro-structure of grinding wheel under SAE20W40. (**b**) Micro-structure of grinding wheel under veg oil. (**c**) Micro-structure of grinding wheel under veg oil + TiO_2.

Further, a good bearing in the grinding region is provided by the spherical appearance and nano-size of the TiO_2 nano-particles. The contact area between the workpiece and grains is narrowed, thereby reducing grain wear flattening; friction pair direct contact is prevented, and the friction between the workpiece and abrasive grains is changed from sliding friction to rolling friction by the TiO_2 nano-particles. The wear rate of the grinding wheel and consumption of energy are lower due to the reduction in the force ratio. The presence of TiO_2 nano-particles is proven by the existence of elemental Ti and O on the abrasive grain surface through the confirmation from SEM and EDS analysis. A lubricating film is formed by TiO_2 nano-particles under external pressure and temperature.

3.6. AFM Analysis of Surface Roughness

Surface roughness is quantitatively measured, and the nano-texture of the nano-composite surface is visualized through atomic force microscopic analysis [58]. Figure 12 represents the three-dimensional AFM image of MMNC using SAE20W40, cashew nutshell oil and cashew nutshell oil with Nano-TiO_2, respectively. The average surface roughness of MMNC using Nano-TiO_2 as lubricating oil is observed to decrease from 226.5 nm to 108.3 nm. The air stream in the MQL system eases the dispersion of TiO_2 nano-particles in the contact region of abrasive grits and metal. The interaction between the cashew nutshell oil and MMNC supports the formation of an appropriate lubrication film, which provides a viscose medium for solid TiO_2 nano-particles. This condition improves the rolling action of nano-particles and results in the improved surface quality of MMNC through the creation of a smooth surface. Mohammadreza et al. found that, in CuO nano-fluid MQL grinding, the rolling action of the nano-particles generates a smooth surface even at a high depth of cut and linear velocity of the workpiece [21]. Hence, it is confirmed from the AFM analysis that the resistance against surface roughness for MMNC is improved by using Nano-TiO_2 in the MQL system.

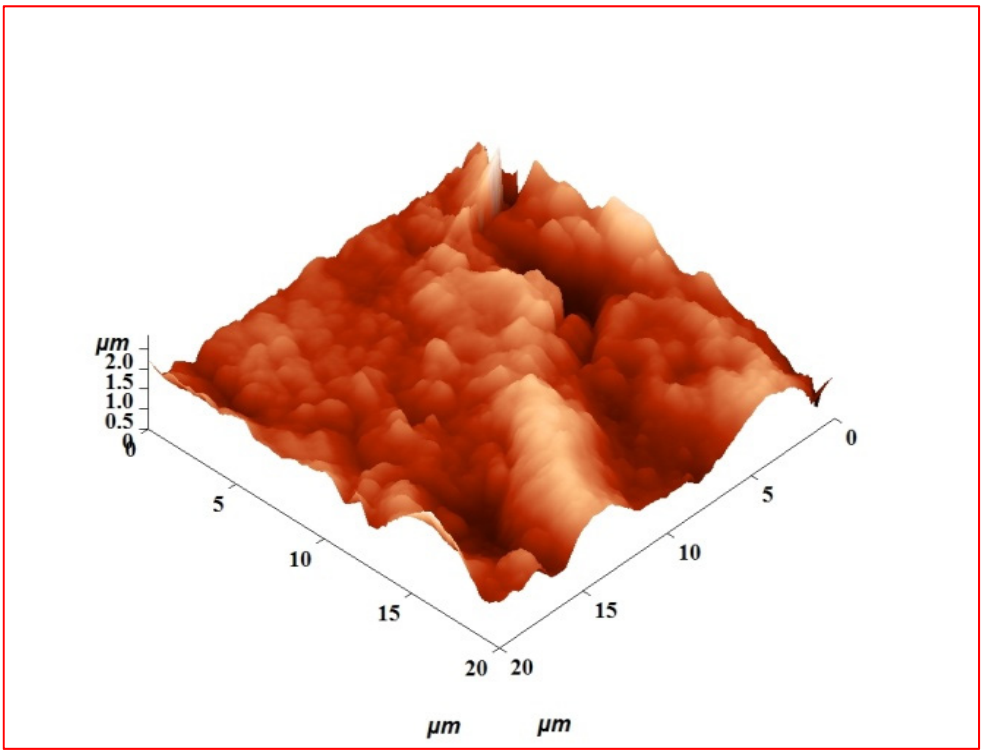

(**a**)

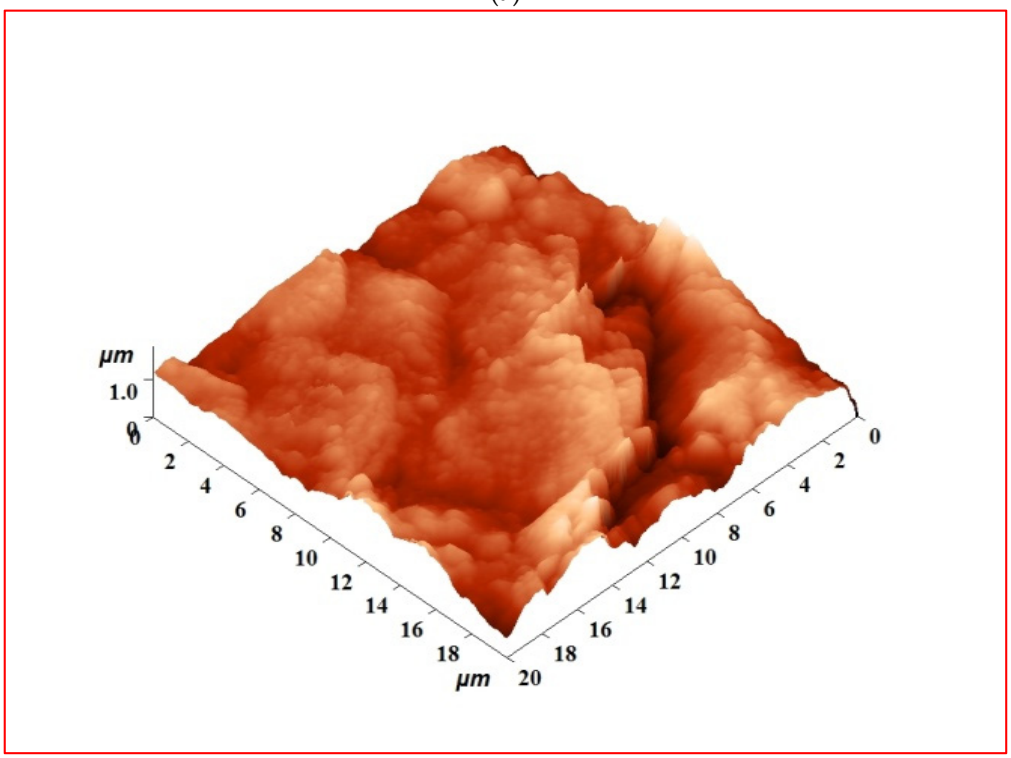

(**b**)

Figure 12. *Cont.*

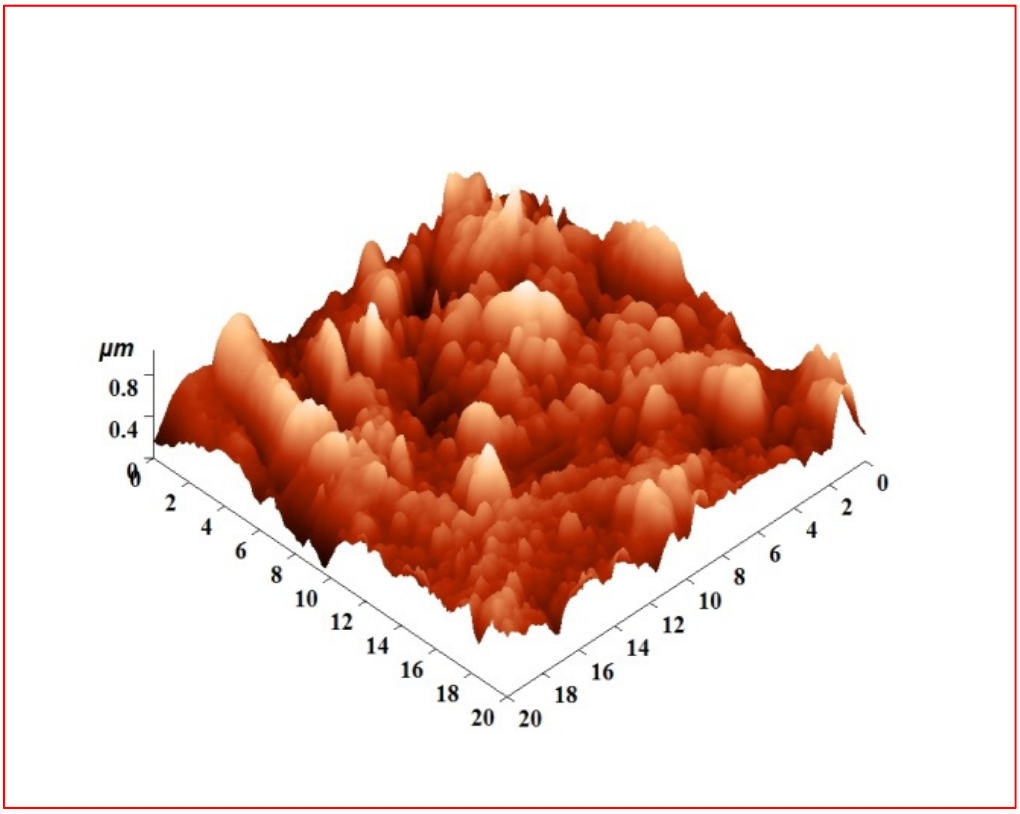

(**c**)

Figure 12. (**a**) AFM analysis of machined surface under SAE20W40. (**b**) AFM analysis of machined surface under veg oil. (**c**) AFM analysis of machined surface under veg oil + TiO_2.

4. Conclusions

The present paper deals with the investigation and optimization of machining parameters, such as the wheel speed, speed of the workpiece, depth of cut and wt % of nano-SiC particles, under different MQL environments, such as SAE20W40, cashew nutshell oil and cashew nutshell oil + Nano-TiO_2, in the grinding of Al matrix nano-composites. The major conclusions drawn from the present investigation are as follows:

- Aluminum matrix nano-composites reinforced by nano-SiC are successfully synthesized using an ultrasonic cavitation-based solidification process, and the characterization of nano-composites is performed using SEM with EDX and IR spectroscopy.
- The properties of the nano-filled lubricant are compared with SAE20W40 and cashew nutshell oil. An improvement in the properties is observed in Tio_2 mixed cashew-nut-based vegetable oil. The wear scar diameter is very low in veg oil + TiO_2 compared to SAE20W40 and veg oil.
- The MQL method is utilized economically in the grinding process, decreasing the coefficient of friction, providing diffusion of oil mist in the machining interface and reducing the tangential forces considerably.
- The ABC algorithm is employed to optimize the sustainable grinding factors of composites reinforced with nano-SiC particles. The results of the optimization technique determine that the following parameters (wheel speed = 910 rpm, depth of cut = 29.42 μm, wt % of nano-SiC = 2.9, workpiece speed = 78 rpm, MQL type = veg oil + TiO_2) are favorable for reducing the cutting force, temperature and surface roughness.
- Nano-fluid MQL reveals a reduction in the cutting force and temperature. The addition of Nano-TiO_2 in cashew nutshell oil improves the performance through enhanced cooling effects and lubrication by their greater diffusion and entrapment at the contact zone.

- A lubricating film layer of the TiO_2 nano-fluid can be formed on the abrasive grain surfaces through chemical and physical reactions of the nano-fluids. The wear flattening generation is prevented and effectively forced to drop from the abrasive grains by this layer.
- It is distinctly clear from the micro-graph that the nano-SiC particles are disintegrated and dragged away from the surface. The difference in thermal expansion among the nano-SiC particles and Al generates heat, resulting in the formation of micro-cracks on the machined surface.

Author Contributions: A.N. Preparation of Composites and complete machining part, T.R. Surface Integrity Analysis S.V. Morphology analysis; D.V. Artificial Bee Colony (ABC) algorithm. All authors have read and agreed to the published version of the manuscript.

Funding: This research received no external funding.

Institutional Review Board Statement: Not applicable.

Informed Consent Statement: The authors affirm that there is no external data and images incorporated in the present project for publication. Informed consent was obtained from all individual authors included in the present study.

Data Availability Statement: There is no data available in this project.

Conflicts of Interest: All authors have no conflict of interest to report. Ensure that accepted principles of ethical and professional conduct have been followed in the present research.

References

1. Peralta, E.; Álvarez, M.; Bárcena, M.M.; González, F.A. On the sustainability of machining processes. Proposal for a unified framework through the triple bottom-line from an understanding review. *J. Clean. Prod.* **2016**, *142*, 3890–3904. [CrossRef]
2. Rajemi, M.F.; Mativenga, P.T.; Aramcharoen, A. Sustainable machining: Selection of optimum turning conditions based on minimum energy considerations. *J. Clean. Prod.* **2010**, *18*, 1059–1065. [CrossRef]
3. Vijayabhaskar, S.; Rajmohan, T. Experimental Investigation and Optimization of Machining Parameters in WEDM of Nano-SiC Particles Reinforced Magnesium Matrix Composites. *Silicon* **2019**, *11*, 1701–1716. [CrossRef]
4. Pawar, P.J.; Vidhate, U.S.; Khalkar, M.Y. Improving the quality characteristics of abrasive water jet machining of marble material using multi-objective artificial bee colony algorithm. *J Comput. Des. Eng.* **2018**, *5*, 319–328. [CrossRef]
5. Rajmohan, T.; Palanikumar, K. Modelling and analysis of performances in drilling hybrid metal matrix composites using D-optimal design. *Int. J. Adv. Manuf. Technol.* **2013**, *64*, 1249–1261. [CrossRef]
6. Rajmohan, T.; Palanikumar, K.; Prakash, S. Grey-fuzzy algorithm to optimise machining parameters in drilling of hybrid metal matrix composites. *Compos. Part B Eng.* **2016**, *50*, 297–308. [CrossRef]
7. Josyula, S.K.; Narala, S.K.R.; Charan, E.G.; Kishawy, H.A. Sustainable Machining of Metal Matrix Composites Using Liquid Nitrogen. *Procedia CIRP* **2016**, *40*, 568–573. [CrossRef]
8. Nandakumar, A.; Rajmohan, T.; Vijayabhaskar, S. Experimental Evaluation of the Lubrication Performance in MQL Grinding of Nano SiC Reinforced Al Matrix Composites. *Silicon* **2019**, *11*, 2987–2999. [CrossRef]
9. Krolczyk, G.M.; Maruda, R.W.; Krolczyk, J.B.; Wojciechowski, S.; Mia, M.; Nieslony, P.; Budzik, G. Ecological trends in machining as a key factor in sustainable production—A review. *J. Clean. Prod.* **2019**, *218*, 601–615. [CrossRef]
10. Li, M.; Yu, T.; Yang, L.; Li, H.; Zhang, R.; Wang, W. Parameter optimisation during minimum quantity lubrication milling of TC4 alloy with grapheme-dispersed vegetable-oil based cutting fluid. *J. Clean. Prod.* **2019**, *209*, 1508–1522. [CrossRef]
11. Mia, M.; Gupta, M.K.; Lozano, J.A.; Carou, D.; Pimenov, D.Y.; Krolczyk, G.; Khan, A.M.; Dhar, N.R. Multi-objective optimization and life cycle assessment of eco-friendly cryogenic N_2 assisted turning of Ti-6Al-4V. *J. Clean. Prod.* **2019**, *210*, 121–133. [CrossRef]
12. Gajrani, K.K.; Suvin, P.S.; Kailas, S.V.; Sankar, M.R. Hard machining performance of indigenously developed green cutting fluid using flood cooling and minimum quantity cutting fluid. *J. Clean. Prod.* **2019**, *206*, 108–123. [CrossRef]
13. Ni, J.; Yang, Y.; Wu, C. Assessment of water-based fluids with additives in grinding disc cutting process. *J. Clean. Prod.* **2019**, *212*, 593–601. [CrossRef]
14. Yin, G.; Wang, D.; Cheng, J. Experimental investigation on micro-grinding of SiCp/Al metal matrix composites. *Int. J. Adv. Manuf. Technol.* **2019**, *102*, 3503–3517. [CrossRef]
15. Rudrapati, R.; Pal, P.K.; Bandyopadhyay, A. Modeling and optimization of machining parameters in cylindrical grinding process. *Int. J. Adv. Manuf. Technol.* **2016**, *82*, 2167–2182. [CrossRef]
16. Haq MA, U.; Khan, A.M.; Gong, L.; Xu, T.; Meng, L.; Hussain, S. A comparative study of face milling of D2 steel using AL2O3 based Nanofluid Minimum Quantity Lubrication and Minimum Quantity Lubrication. *J. Adv. Sci. Tecnol. Res.* **2018**, *12*, 99–105.

17. Thiagarajan, C.; Sivaramakrishnan, R.; Somasundaram, S. Cylindrical grinding of sic particles reinforced aluminium metal matrix composites. *J. Eng. Appl. Sci.* **2011**, *6*, 14–20.
18. Wang, Y.; Li, C.; Zhang, Y.; Yang, M.; Li, B.; Jia, D.; Hou, Y.; Mao, C. Experimental evaluation of the lubrication properties of the wheel/workpiece interface in MQL grinding using different types of vegetable oils. *J. Clean. Prod.* **2016**, *127*, 488–499. [CrossRef]
19. Gajrani, K.K.; Ram, D.; Sankar, M.R. Biodegradation and hard machining performance comparison of eco-friendly cutting fluid and mineral oil using flood cooling and minimum quantity cutting fluid techniques. *J. Clean. Prod.* **2017**, *165*, 1420–1435. [CrossRef]
20. Ashwani, P.; Patral, K.; Dyakonov, A.A. A comprehensive review of micro-grinding: Emphasis on toolings, performance analysis, modeling techniques, and future research directions. *Int. J. Adv. Manuf. Technol.* **2019**, *104*, 63–102.
21. Shabgard, M.; Seyedzavvar, M.; Mohammadpourfard, M. Experimental investigation into lubrication properties and mechanism of vegetable-based CuOnanofluid in MQLgrinding. *Int. J. Adv. Manuf. Technol.* **2017**, *92*, 3807–3823. [CrossRef]
22. Zhang, X.; Li, C.; Zhang, Y.; Jia, D.; Li, B.; Wang, Y.; Yang, M.; Hou, Y.; Zhang, X. Performances of Al2O3/SiC hybrid nanofluids in minimum-quantity lubrication grinding. *Int. J. Adv. Manuf. Technol.* **2016**, *86*, 3427–3441. [CrossRef]
23. Zhang, X.; Li, C.; Jia, D.; Gao, T.; Zhang, Y.; Yang, M.; Li, R.; Ha, Z.; Ji, H. Spraying parameter optimization and microtopography evaluation in nanofluid minimum quantity lubrication grinding. *Int. J. Adv. Manuf. Technol.* **2019**, *103*, 2523–2539. [CrossRef]
24. Zhu, G.; Yuan, S.; Chen, B. Numerical and experimental optimizations of nozzle distance in minimum quantity lubrication (MQL) milling process. *Int. J. Adv. Manuf. Technol.* **2019**, *101*, 565–578. [CrossRef]
25. Shen, B.; Shih, A.J. Minimum quantity lubrication (mql) grinding using vitrified cbn wheels. *Trans. NAMRI/SME* **2009**, *37*, 129–136.
26. Prabhu, S.; Vinayagam, B.K. AFM investigation in grinding process with nanofluids using Taguchi analysis. *Int. J. Adv. Manuf. Technol.* **2012**, *60*, 149–160. [CrossRef]
27. Setti, D.; Ghosh, S.; Rao, P.V. Application of Nano Cutting Fluid under Minimum Quantity Lubrication (MQL) Technique to Improve Grinding of Ti–6Al–4V Alloy. *Int. J. Mech. Mechatron. Eng.* **2012**, *6*, 10.
28. Adibi, H.; Esmaeili, H.; Rezaei, S.M. Study on minimum quantity lubrication (MQL) in grinding of carbon fiber-reinforced SiC matrix composites (CMCs). *Int. J. Adv. Manuf. Technol.* **2017**, *95*, 3753–3767. [CrossRef]
29. Chinchanikar, S.; Choudhury, S.K. Hard turning using HiPIMS-coated carbide tools: Wear behavior under dry and minimum quantity lubrication (MQL). *Measurement* **2014**, *55*, 536–548. [CrossRef]
30. Tawakoli, T.; Hadad, M.J.; Sadeghi, M.H.; Daneshi, A.; Stockert, S.; Rasifard, A. An experimental investigation of the effects of workpiece and grinding parameters on minimum quantity lubrication (MQL) grinding. *Int. J. Mach. Tools Manuf.* **2009**, *49*, 924–932. [CrossRef]
31. Mao, C.; Tang, X.; Zou, H.; Huang, X.; Zhou, Z. Investigation of Grinding Characteristic using Nanofluid Minimum Quantity Lubrication. *Int. J. Precis. Eng. Manuf.* **2010**, *13*, 1745–1752. [CrossRef]
32. Mao, C.; Zou, H.; Huang, X.; Zhang, J.; Zhou, Z. The influence of spraying parameters on grinding performance for nanofluid minimum quantity lubrication. *Int. J. Adv. Manuf. Technol.* **2013**, *64*, 1791–1799. [CrossRef]
33. Lee, P.; Nam, J.S.; Li, C.; Lee, S.W. An Experimental Study on Micro-Grinding Process with Nanofluid Minimum Quantity Lubrication (MQL). *Int. J. Precis. Eng. Manuf.* **2012**, *13*, 331–338. [CrossRef]
34. Sadeghi, M.H.; Hadad, M.J.; Tawakoli, T.; Vesali, A. An investigation on surface grinding of AISI 4140 hardened steel using minimum quantity lubrication-MQL technique. *Int. J. Mater. Form.* **2010**, *3*, 241–251. [CrossRef]
35. Sani AS, A.; Rahim, E.A.; Sharif, S.; Sasahara, H. Machining performance of vegetable oil with phosphonium- and ammonium-based ionic liquids via MQL technique. *J. Clean. Prod.* **2019**, *209*, 947–964. [CrossRef]
36. Ni, H.-M.; Liu, Y.-J.; Fan, Y.-C. Optimization of injection scheme to maximizing cumulative oil steam ratio based on improved artificial bee colony algorithm. *J. Pet. Sci. Eng.* **2019**, *173*, 371–380. [CrossRef]
37. Stachurski, W.; Sawicki, J.; Wojcik, R.; Nadolny, K. Influence of application of hybrid MQL-CCA method of applying coolant during hob cutter sharpening on cutting blade surface condition. *J. Clean. Prod.* **2018**, *171*, 892–910. [CrossRef]
38. Dogra, M.; Sharma, V.S.; Dureja, J.S.; Gill, S.S. Environment-friendly technological advancements to enhance the sustainability in surface grinding—A review. *J. Clean. Prod.* **2018**, *197*, 218–231. [CrossRef]
39. Zhang, J.; Li, C.; Zhang, Y.; Yang, M.; Jia, D.Z.; Liu, G.; Hou, Y.; Li, R.; Zhang, N.; Wu, Q.; et al. Experimental assessment of an environmentally friendly grinding process using Nanofluid minimum quantity lubrication with cryogenic air. *J. Clean. Prod.* **2018**, *193*, 236–248. [CrossRef]
40. Rapeti, P.; Pasam, V.K.; Gurram KM, R.; Revuru, R.S. Performance evaluation of vegetable oil-based Nano cutting fluids in machining using grey relational analysis—A step towards sustainable manufacturing. *J. Clean. Prod.* **2018**, *172*, 2862–2875. [CrossRef]
41. Lee, P.H.; Kim, J.W.; Lee, S.W. Experimental characterization on eco-friendly micro-grinding process of titanium alloy using air flow assisted electrospray lubrication with Nano fluid. *J. Clean. Prod.* **2018**, *201*, 452–462. [CrossRef]
42. Pashmforoush, F.; Bagherinia, R.D. Influence of water-based copper Nano fluid on wheel loading and surface roughness during grinding of Inconel 738 super alloy. *J. Clean. Prod.* **2018**, *178*, 363–372. [CrossRef]
43. Mia, M.; Gupta, M.K.; Singh, G.; Krolczyk, G.; Pimenov, D.Y. An approach to cleaner production for machining hardened steel using different cooling-lubrication conditions. *J. Clean. Prod.* **2018**, *187*, 1069–1081. [CrossRef]

44. Kleinová, A.; Huran, J.; Sasinková, V.; Perný, M.; Šály, V.; Packa, J. FTIR spectroscopy of silicon carbide thin films prepared by PECVD technology for solar cell application. In *Reliability of Photovoltaic Cells, Modules, Components, and Systems*; SPIE: Bellingham, WA, USA, 2015. [CrossRef]
45. Baskar, S.; Sriram, G.; Arumugam, S. Experimental Analysis on Tribological Behavior of Nano Based Bio-Lubricants Using Four-Ball Tribometer. *Tribol. Ind.* **2015**, *37*, 449–454.
46. Su, Y.; Gong, L.; Li, B.; Liu, Z.; Chen, D. Performance evaluation of nanofluidMQL with vegetable-based oil and ester oil as base fluids in turning. *Int. J. Adv. Manuf. Technol.* **2016**, *83*, 2083–2089. [CrossRef]
47. Lakshmanan, P.; Kalaichelvan, K.; Sornakumar, T. Processing and Performance Characteristics of Aluminum-Nano Boron Carbide Metal Matrix Nanocomposites. *Mater. Manuf. Process.* **2015**, *31*, 1275–1285.
48. Barczak, L.M.; Batako, A.D. Application of Minimum Quantity Lubrication in Grinding. *Mater. Manuf. Process.* **2012**, *27*, 406–411. [CrossRef]
49. Sun, F.H.; Li, X.K.; Wang, Y.; Chen, M. Studies on the Grinding Characteristics of SiC Particle Reinforced Aluminum-based MMCs. *Key Eng. Mater.* **2006**, *304–305*, 261–265. [CrossRef]
50. Kumar, D.; Rajmohan, T. Experimental investigation of wear of multiwalled carbon nanotube particles-filled poly-ether-ether-ketone matrix composites under dry sliding. *J. Thermoplast. Compos. Mater.* **2019**, *32*, 521–543. [CrossRef]
51. Hadad, M.J.; Tawakoli, T.; Sadeghi, M.H.; Sadeghi, B. Temperature and energy partition in minimum quantity lubrication-MQL grinding process. *Int. J. Mach. Tools Manuf.* **2012**, *54*, 10–17. [CrossRef]
52. Gupta, M.K.; Sood, P.K.; Sharma, V.S. Parameters optimization of titanium alloy using response surface methodology and particle machining swarm optimization under minimum quantity lubrication environment. *Mater. Manuf. Process.* **2015**, *31*, 1671–1682. [CrossRef]
53. Rabiei, F.; Rahim, A.R.; Hadad, M.J.; Ashrafijou, M. Performance improvement of minimum quantity lubrication(MQL) technique in surface grinding by modeling and optimization. *J. Clean. Prod.* **2014**, *86*, 447–460. [CrossRef]
54. Mao, C.; Zhang, J.; Huang, Y.; Zou, H.; Huang, X.; Zhou, Z. Investigation on the Effect of Nanofluid Parameters on MQL Grinding. *Mater. Manuf. Process.* **2013**, *28*, 436–442. [CrossRef]
55. Tiwari, A.K.; Ghosh, P.; Sarkar, J. Investigation of thermal conductivity and viscosity of nanofluids. *J. Environ. Res. Dev.* **2012**, *7*, 768–777.
56. Zhu, C.; Gu, P.; Liu, D.; Hu, X.; Wu, Y. Evaluation of surface topography of SiCp/Al composite in grinding. *Int. J. Adv. Manuf. Technol.* **2019**, *102*, 2807–2821. [CrossRef]
57. Liu, G.; Li, C.; Zhang, Y.; Yang, M.; Jia, D.; Zhang, X.; Guo, S.; Li, R.; Zhai, H. Process parameters optimization and experimental evaluation for nanofluid MQL in grinding Ti-6Al-4V based on grey relational analysis. *Mater. Manuf. Process.* **2017**, *33*, 950–963. [CrossRef]
58. Rajesh Kumar, B.; Subba Rao, T. AFM Studies on surface morphology, topography and texture of nanostructured zinc aluminium oxide thin films. *Dig. J. Nanomater. Biostruct.* **2012**, *7*, 1881–1889.